

Cuboidal [Ni₄O₄] cluster as a precursor to recyclable, carbon-supported nickel nanoparticle reduction catalysts

Yan-Qiu Yuan,^a Feng-Ling Yuan,^a Fei-Long Li,^a Zhi-Min Hao,^a Jun Guo,^a David J. Young,^{*c} Wen-Hua Zhang^{*a} and Jian-Ping Lang^{*ab}

^a College of Chemistry, Chemical Engineering and Materials Science, Soochow University, Suzhou 215123, Jiangsu, P. R. China; E-mail: whzhang@suda.edu.cn; jplang@suda.edu.cn

^b State Key Laboratory of Organometallic Chemistry, Shanghai Institute of Organic Chemistry, Chinese Academy of Sciences, Shanghai 200032, P. R. China.

^c Faculty of Science, Health, Education and Engineering, University of the Sunshine Coast, Maroochydore, Queensland 4558, Australia; E-mail: dyoung1@usc.edu.au

Table of Contents

- 1. Synthetic procedures of the ligand and compounds 1 – 4**
- 2. X-ray structure determination for 1 – 4**
- 3. Structural discussion of 2 – 4**
- 4. Procedure for the reduction of 4-nitrophenol (4-NP) to 4-aminophenol (4-AP) monitored by UV-vis**
- 5. Procedure for the reduction of 4-nitrophenol (4-NP) to 4-aminophenol (4-AP) in 1 mmol scale**
- 6. Preparation of Ni-free carbon nanoparticles from NiNPs/C-450**
- 7. Figures S1 – S11**
- 8. Tables S1 – S5**
- 9. Original ¹H NMR, ¹³C NMR, TOF-Mass, ESI-Mass, and IR spectra of HL and compounds 1 – 4**

1. Synthetic procedures of the ligand and compounds 1 – 4

Materials

The ligand (5-(4-(tert-butyl)phenyl)pyridine-2-yl)methanol (HL) was prepared according to the literature method.¹ Other chemicals and reagents were obtained from commercial sources and used without further purification. IR spectra (KBr disk, 400–4000 cm^{-1}) were recorded on a Perkin-Elmer 1320 spectrometer. Elemental analyses for C, H and N were carried out on a Carlo-Erba CHNO-S microanalyzer. A BTF-1200C-S quartz tube furnace was employed for carbonization. Thermogravimetric analysis (TGA) was performed with a Mettler Toledo Star system (heating rate of 5 $^{\circ}\text{C}\cdot\text{min}^{-1}$). The powder X-ray diffraction (PXRD) measurements were carried out on a PANalytical X'Pert PRO MPD system (PW3040/60). UV-vis absorption spectra were obtained on a Varian Cary-50 UV-visible spectrophotometer. ^1H and ^{13}C NMR spectra in DMSO were recorded at r.t. on a Varian UNITY plus-400 spectrometer and chemical shifts are referenced to residual DMSO (2.50 ppm for ^1H and 39.5 ppm for ^{13}C). High-resolution mass spectra (HRMS-ESI) were obtained on a MicroTM or a Micro YA263 Q-TOF mass spectrometer. Melting points were recorded on a Mel-Temp II apparatus. Transmission electron microscopy (TEM) was carried out on a HITACHI HT-7700 electron microscope operated at 120 kV. High-resolution transmission electron microscopy (HRTEM) was performed on an FEI Tecnai G20 electron microscope operated at 200 kV. X-ray photoelectron spectroscopy (XPS) was accomplished using an SSI S-Probe XPS spectrometer. Raman spectra were obtained on a Confocal LabRAM HR800 spectrometer with a laser excitation wavelength of 632.8 nm. Magnetic measurements were performed on an MPMS-SQUID-VSM system at 300 K. The porosity measurements were performed on Belsorp surface area and porosity analysis instrument at 77 K. The Brunauer-Emmett-Teller (BET) method was utilized to calculate the specific surface areas. All samples were degassed at 150 $^{\circ}\text{C}$ for 12 h before the measurement.

Synthesis of methyl 5-(4-(tert-butyl)phenyl)picolinate

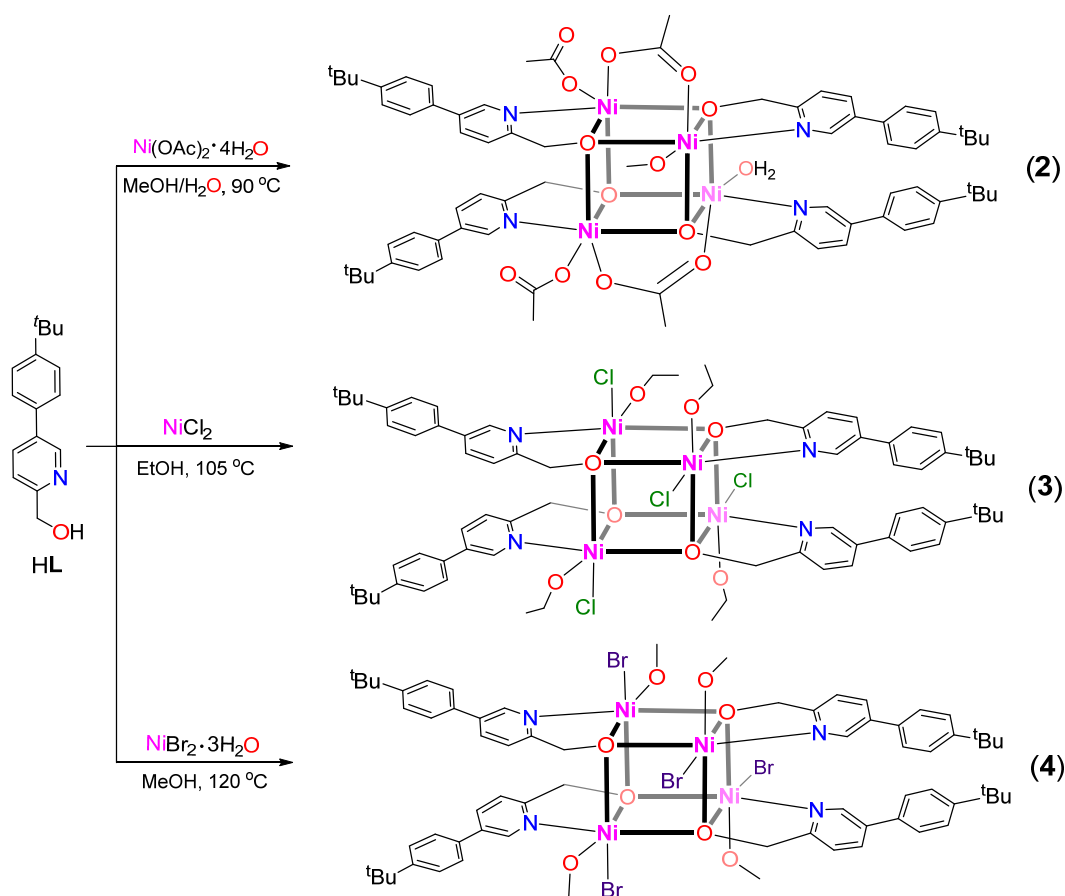
4-tert-Butylphenylboronic acid (534 mg, 3 mmol), 5-bromopyridine-2-carboxylic acid

methylester (432 mg, 2 mmol) and K_2CO_3 (552 mg, 4 mmol) were mixed together in a 50 mL double-necked flask and $\text{Pd}(\text{PPh}_3)_4$ (46 mg, 0.04 mmol, 2 mol %) was then quickly added. The air in the flask was exchanged with N_2 three times followed by addition of 10 mL degassed toluene. The resulting mixture was heated at 110 °C for 48 h under an N_2 atmosphere. Toluene was then removed under reduced pressure. The resulting dark brown mixture was extracted with brine and ethyl acetate 3 times and the organic layers combined and dried over anhydrous Na_2SO_4 . The solvent was evaporated and the resulting brown residue purified on a silica column with n-hexane/ethyl acetate ($v/v = 6:1$, $R_f = 0.33$) to yield the title compound as a fine yellow powder. Yield: 510 mg (94 %). Anal. calcd (%) for $\text{C}_{17}\text{H}_{19}\text{NO}_2$: C 75.79, H 7.06, N 5.20; found: C 75.63, H 7.16, N 5.07. m.p.: 135.5 – 136.2 °C. HRMS (ESI-TOF) m/z : Calcd. for $\text{C}_{17}\text{H}_{20}\text{NO}_2$ $[\text{M} + \text{H}]^+$: 270.1416, found: 270.1498. IR (KBr disc): 2955(s), 1739(s), 1515(m), 1398(w), 1372(s), 1236(m), 1190(m), 1140(s), 1515(m), 1116(s), 832(s), 797(s), 770(w), 743(w). ^1H NMR ($\text{DMSO}-d_6$, 400 MHz): δ 9.12 (s, 1H), 8.35 (d, $J = 8.1$ Hz, 1H), 8.20 (d, $J = 8.1$ Hz, 1H), 7.83 (d, $J = 8.1$ Hz, 2H), 7.65 (d, $J = 8.1$ Hz, 2H), 3.99 (s, 3H), 1.41 (s, 9H) ppm. ^{13}C NMR ($\text{DMSO}-d_6$, 101 MHz): δ 165.1, 151.6, 147.7, 145.9, 138.4, 134.8, 133.0, 126.9, 126.1, 125.0, 52.4, 34.4, 31.0 ppm.

Synthesis of (5-(4-(tert-butyl)phenyl)pyridine-2-yl)methanol (HL)

Absolute EtOH (100 mL) was added to a 150 mL triple-necked flask in an ice bath and degassed with N_2 for 30 minutes. Methyl 5-(4-(tert-butyl)phenyl)picolinate (807 mg, 3 mmol) and NaBH_4 (91 mg, 2.4 mmol) were then added in sequence with stirring, followed by portion-wise addition of CaCl_2 (333 mg, 3 mmol) over 5 minutes. The reaction was placed in ice bath for 5 h and monitored with thin-layer chromatography. The reaction was quenched with concentrated H_2SO_4 by adjusting the pH value to 3 – 4 and left to stand overnight at r.t. before filtration. The solid residue was extracted with absolute EtOH. The combined EtOH extracts were evaporated to obtain a white solid that was dissolved in brine and further extracted three time with CH_2Cl_2 . The organic layers were combined and dried over anhydrous Na_2SO_4 . Evaporation of the solvent

provided a white powder that was purified by silica gel column chromatography with petroleum ether/ethyl acetate ($v/v = 2:1$, $R_f = 0.41$) to yield the title compound as a fine white powder. Yield: 300 mg (41 %). Anal. calcd (%) for $C_{16}H_{19}NO$: C 79.62, H 7.88, N 5.81; found: C 78.59, H 7.86, N 5.67. m.p.: 142.9 – 143.5 °C. HRMS (ESI-TOF) m/z : Calcd. for $C_{16}H_{20}NO$ $[M + H]^+$: 242.1467, found: 242.1550. IR (KBr disc): 3372(w), 2920(w), 1524(w), 1456(m), 1336(s), 1259(m), 1215(m), 848(w), 826(s), 747(w), 718(w). 1H NMR (DMSO- d_6 , 400 MHz): δ 8.77 (s, 1H), 8.05 (d, $J = 8.0$ Hz, 1H), 7.64 (d, $J = 8.2$ Hz, 2H), 7.52 (t, 3H, $J = 9.2$ Hz), 5.45 (t, $J = 5.8$ Hz, 1H), 4.60 (d, $J = 5.8$ Hz, 2H), 1.31 (s, 9H) ppm. ^{13}C NMR (DMSO- d_6 , 101 MHz): δ 160.6, 150.4, 146.4, 134.3, 134.3, 133.6, 126.4, 125.9, 120.2, 64.1, 34.3, 31.1 ppm.



Scheme S1. Synthesis of compounds **2** – **4** from Ni salts and HL.

Synthesis of $[Ni_4L_4(\mu-HCOO)_2(HCOO)_2(H_2O)_2] \cdot H_2O$ (**1**)

A mixture of $Ni(NO_3)_2 \cdot 6H_2O$ (60 mg, 0.2 mmol) and HL (24 mg, 0.1 mmol) in 10 mL DMF/ H_2O ($v/v = 1:1$) solvent was placed in a pressure tube. The tube was sealed

and heated at 120 °C for 72 h, followed by smooth cooling to r.t. over 48 h. Green block crystals of **1** were collected by filtration, washed with Et₂O and dried in air. Yield: 24 mg (67.13 % based on HL). Anal. calcd (%) for C₆₈H₈₄N₄Ni₄O₁₄: C 57.05, H 5.87, N 3.91; found: C 57.04, H 5.95, N 4.10. IR (KBr disc, cm⁻¹): 3412(s), 3030(w), 1615(s), 1578(s), 1447(w), 1382(m), 1270(w), 1231(w), 1201(w), 1043(w), 815(m), 777(w), 742(w). ESI-MS m/z: Calcd. for [Ni₄L₄(HCOO)₃]⁺: 1329.29, found: 1329.15 (Fig. S4a). Correct assignment of the protons from the ¹H NMR (Fig. S21) cannot be done due the paramagnetic nature of the product.

Synthesis of [Ni₄L₄(μ-OAc)₂(OAc)₂(H₂O)(MeOH)]·2H₂O·2MeOH (**2**)

Ni(OAc)₂·4H₂O (25 mg, 0.1 mmol) and HL (24 mg, 0.1 mmol) were dissolved in a 10 mL MeOH/H₂O mixed solvent (v / v = 1 : 1). The reactants were sealed in a pressure tube, heated at 90 °C for 72 h, followed by smooth cooling to r.t. over 48 h. Green block crystals were washed with cold MeOH/H₂O (v / v = 1 : 1) and dried overnight in air. Yield: 20 mg (50.55 % based on Ni). Anal. calcd (%) for C₁₅₀H₂₀₄N₈Ni₈O₃₆: C 56.87, H 6.45, N 3.54; found: C 56.55, H 6.48, N 3.87. IR (KBr disk, cm⁻¹): 3424(s), 2964(m), 1571(s), 1414(s), 1384(s), 1293(m), 1270(w), 1114(s), 1045(m), 820(m), 760(w), 728(w). ESI-MS m/z: Calcd. for [Ni₄L₄(OAc)₂(OH)]⁺: 1329.32, found: 1329.16 (Fig. S4b). Correct assignment of the protons from the ¹H NMR (Fig. S22) cannot be done due the paramagnetic nature of the product.

Synthesis of [Ni₄L₄(EtOH)₄Cl₄] (**3**)

NiCl₂ (26 mg, 0.1 mmol), HL (48 mg, 0.2 mmol) and sodium butyrate (22 mg, 0.2 mmol) were dissolved in 10 mL EtOH. The clear green liquid was sealed in a pressure tube, heated at 105 °C for 72 h followed by smooth cooling to r.t. over 48 h. Green crystals were collected by filtration, washed with a small quantity of EtOH and dried in air. Yield: 12 mg (31.37 % based on Ni). Anal. calcd (%) for C₇₂H₉₆Cl₄N₄Ni₄O₈: C 56.76, H 6.31, N 3.68; found: C 56.25, H 6.45, N 3.60. IR (KBr disk, cm⁻¹): 3424(s), 2962(s), 1613(m), 1399(s), 1384(s), 1293(w), 1270(w), 1045(s), 821(m), 729(w), 728(w). ESI-MS m/z: Calcd. for {[Ni₄L₄Cl₄(EtOH)₅(H₂O)₃] + 2H⁺}²⁺: 811.71, found:

811.73 (Fig. S4c). Correct assignment of the protons from the ^1H NMR (Fig. S23) cannot be done due the paramagnetic nature of the product.

Synthesis of $[\text{Ni}_4\text{L}_4(\text{MeOH})_4\text{Br}_4]$ (**4**)

$\text{NiBr}_2 \cdot 3\text{H}_2\text{O}$ (55 mg, 0.2 mmol) and **HL** (48 mg, 0.2 mmol) was dissolved in 10 mL of MeOH. The green clear solution was sealed in a pressure tube, heated at 120 °C for 72 h before smooth cooling to r.t. over 48 h. Green crystals were collected by filtration, washed with a small quantity of MeOH and dried in air. Yield: 31 mg (37.80 % based on Ni). Anal. calcd (%) for $\text{C}_{63}\text{H}_{88}\text{N}_4\text{Ni}_4\text{O}_8$: C 46.10, H 5.35, N 3.42; found: C 45.90, H 5.31, N 3.44. IR (KBr disk, cm^{-1}): 3423(s), 3031(w), 1610(m), 1447(w), 1384(m), 1363(m), 1236(w), 1236(w), 1045(s), 821(m), 743(w), 728(w). ESI-MS m/z : Calcd. for $\{[\text{Ni}_2\text{L}_2\text{Br}_3(\text{MeOH})(\text{DMF})_2(\text{H}_2\text{O})] + 2\text{H}^+\}^+$: 1033.06, found: 1032.83 (Fig. S4d). Correct assignment of the protons from the ^1H NMR (Fig. S24) cannot be done due the paramagnetic nature of the product.

Synthetic procedure for NiNPs/C

In a typical experiment, compound **1** was added to a ceramic boat and carefully loaded into a quartz tube furnace. The sample was subjected to a smooth flow of N_2 for 30 minutes to remove O_2 and moisture. This N_2 flow was turned down during heating. The sample was heated from r.t. to T ($T = 450\text{ }^\circ\text{C}$, $500\text{ }^\circ\text{C}$, $550\text{ }^\circ\text{C}$ and $600\text{ }^\circ\text{C}$) at a heating rate of $1\text{ }^\circ\text{C} \cdot \text{min}^{-1}$ and maintained at T for 3 h before evenly cooling to r.t. in a flow of N_2 . The black sample obtained was denoted as NiNPs/C-T.

2. X-ray structure determination for **1** - **4**

All measurements were made on a Bruker D8-Quest (**2**, **3** and **4**) and an Agilent Xcalibur (**1**) CCD X-ray diffractometer using an enhanced X-ray source Mo $\text{K}\alpha$ ($\lambda = 0.71073\text{ \AA}$). Each single crystal was mounted at the top of a glass fiber with grease in a stream of N_2 . Cell parameters were refined using the programs Bruker SAINT (for **2**, **3** and **4**) and *CrysAlisPro* (Agilent Technologies, Ver. 1.171.35.21, 2012) (for **1**). Absorption corrections (multi-scan) were applied.² All crystal structures were solved

by direct methods and refined on F₂ by full-matrix least-squares methods with the SHELXTL-2013 program.³ The tert-butyl groups in the **L** ligands of **1** displayed rotational disorder with the relative ratios of 0.70/0.30, 0.62/0.38, 0.29/0.71 and 0.30/0.70 refined for the two components. The locations of the hydrogen atoms on the water molecules were suggested by the Calc-OH program in the WinGX suite⁴ and their O–H distances further restrained to O–H = 0.83 Å with thermal parameters constrained to $U_{\text{iso}}(\text{H}) = 1.2U_{\text{eq}}(\text{O})$. The location of the two hydrogen atoms on the coordinated EtOH in **3** were suggested by the Calc-OH program in the WinGX suite.⁴ Their coordinates were subsequently fixed and thermal parameters constrained to $U_{\text{iso}}(\text{H}) = 1.2U_{\text{eq}}(\text{O})$. For **4**, part of the two **L** ligands displayed conformational disorder with the relative ratios of 0.42/0.58 and 0.62/0.38 for the two components. Some amount of spatially delocalized electron density in the lattice of **2** – **4** was found but acceptable refinement results could not be obtained. The solvent contribution was then modeled using SQUEEZE in the Platon program suite.⁵ Crystallographic data have been deposited with the Cambridge Crystallographic Data Center (CCDC) (1536067 – 1536070). These data can be either obtained free of charge from the CCDC via www.ccdc.cam.ac.uk/data_request/cif or from the Electronic Supplementary Information (ESI). A summary of crystal data and structure refinement parameters of **1** – **4** are given in Table S1 and the selected bond lengths and angles are listed in Table S2.

3. Structural discussion of **2** – **4**

The cuboidal [Ni₄O₄] skeleton, the relative arrangement of the four **L** ligands, as well as the bridging acetate of **2** (Fig. S1a) resemble that of **1**. There are, however, notable differences of the two structures. For example, although there are two additional monodentate acetate ligands in **2** (versus formate in **1**), these acetate ligands locate within the side plane of the cubane which supports two staggered **L** ligands (versus two monodentate formates in **1** located at the base plane of the cubane). As a consequence, one additional aqua ligand and MeOH ligand coordinated to the two Ni centers within the other side plane of the cubane (versus two aqua ligands in **1**

coordinated to the two Ni centers at the upper plane of the cubane).

Compounds **3** (Fig. S1b) and **4** (Fig. S1c) are structurally similar and only differ in coordination solvates (EtOH in **3** and MeOH in **4**) and outside donor (Cl in **3** and Br in **4**). Take the structure of **3** as an example, all the four Ni centers adopt the same coordination environment and are associated by three μ_3 -O atoms in three orthogonal vectors from three **L** ligands. Its octahedral coordination is filled by one N atom (from one of the three **L** ligands), one terminal Cl⁻ and one EtOH solvate. It is notable that although compounds **1** and **2**, **3** and **4** share similar Ni₄O₄ cluster skeletons, they represent two structural types. A pair of **L** ligands on each of the opposite cuboidal faces exhibit a staggered conformation and these **L** pairs have different orientations. In **1** and **2**, the two **L** ligand pairs are nearly parallel while in **3** and **4**, the two **L** ligand pairs are roughly orthogonal. The Ni···Ni separations for **2** (2.9251(4) – 3.2081(4) Å), **3** (3.0804(11) – 3.1818(11) Å) and **4** (3.1048(17) – 3.1628(16) Å) are comparable to those found in **1** (2.8896(7) – 3.1982(7) Å). While the Ni- μ_3 -O distances for **2** (2.0352(13) – 2.0820(13) Å), **3** (2.039(3) – 2.116(5) Å) and **4** (2.037(7) – 2.119(7) Å) are also similar to those found in **1** (2.043(2) – 2.090(2) Å). Further structural analysis revealed intramolecular hydrogen bonding between coordinated water and monodenate carboxylate (**1**), MeOH and monodenate carboxylate (**2**), EtOH and Cl (**3**), and MeOH and Br (**4**) (Table S3), which may partly explain the formation of such different cuboidal structural types.

4. Procedure for the reduction of 4-nitrophenol (4-NP) to 4-aminophenol (4-AP) monitored by UV-vis

NiNPs/C-T (2 mg) and water (2.05 mL) were added into in a 4.5 mL glass vial and ultra-sonicated for a few minutes to form a suspension. 4-NP (0.3 mL, 1 mM) was added and the light yellow mixture stirred for several minutes (800 rpm) at 20 °C. This light yellow solution immediately became deep yellow upon introducing an aqueous NaBH₄ solution (0.65 mL, 0.2 M) and then gradually became colorless. The conversion process was monitored by UV-vis spectroscopy. The catalyst was separated with a magnet and rinsed with water for subsequent runs.

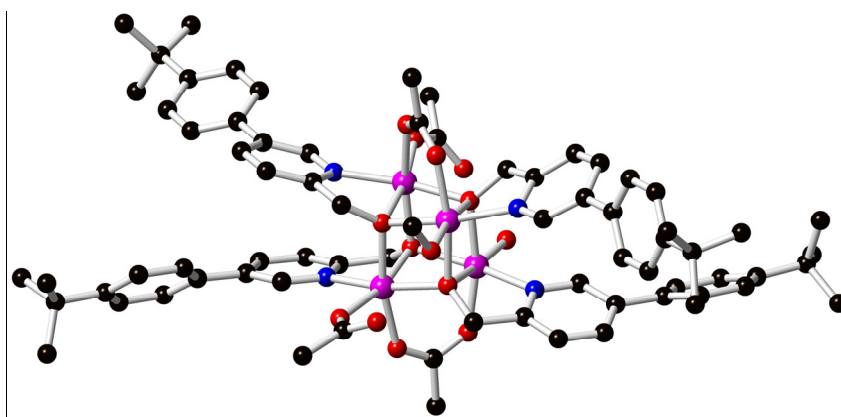
5. Procedure for the reduction of 4-nitrophenol (4-NP) to 4-aminophenol (4-AP) in 1 mmol scale

4-NP (139 mg, 1 mmol) was slowly dissolved in 4 mL of water, and an additional 2 mL water solution containing NaBH₄ (227 mg, 6 mmol) solution was added before adding solid NiNPs/C-450 (10 mg). The mixture stirred for 2 h (800 rpm) at 20 °C. The conversion process was monitored by thin layer chromatography (TLC) and the resulting dark brown mixture extracted with ethyl acetate for 3 times. The organic layer was combined and dried over anhydrous Na₂SO₄. Evaporation of the solvent and purified by silica gel column chromatography with petroleum ether/ethyl acetate ($v/v = 1:1$, $R_f = 0.53$) yielded 4-AP. Yield: 104.20 mg (95.60 %).

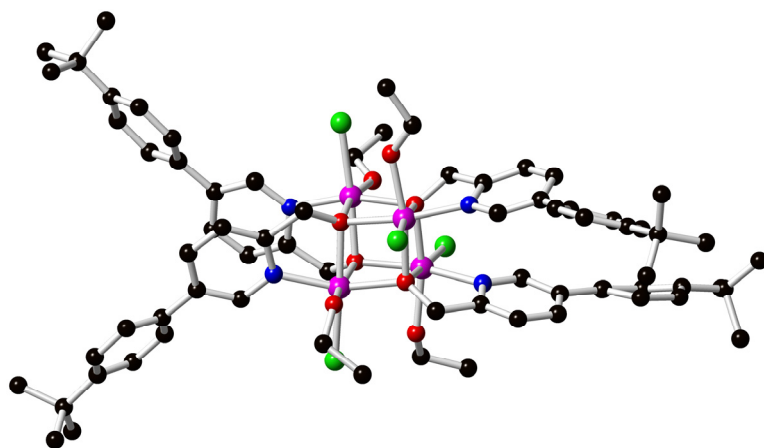
6. Preparation of Ni-free carbon nanoparticles from NiNPs/C-450

40 mg NiNPs/C-450 was mixed with 40 mL HCl (10 M) and the mixture kept stirring overnight at 90 °C. The black solid was filtered off, repeatedly washed with H₂O and EtOH before finally dried in an oven.

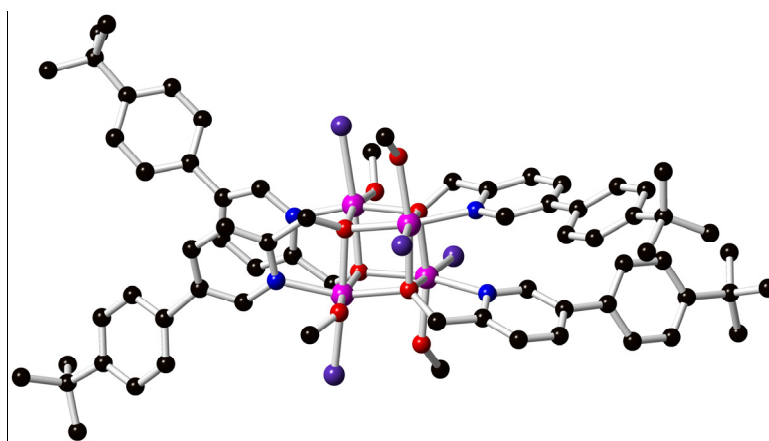
7. Figures S1 – S11



(a)



(b)



(c)

Fig. S1 Structures of **2** (a), **3** (b), and **4** (c) with the disordered components, lattice solvates and hydrogen atoms omitted. Color codes: Ni (magenta), O (red), N (blue), C (black), Cl (green), Br (indigo).

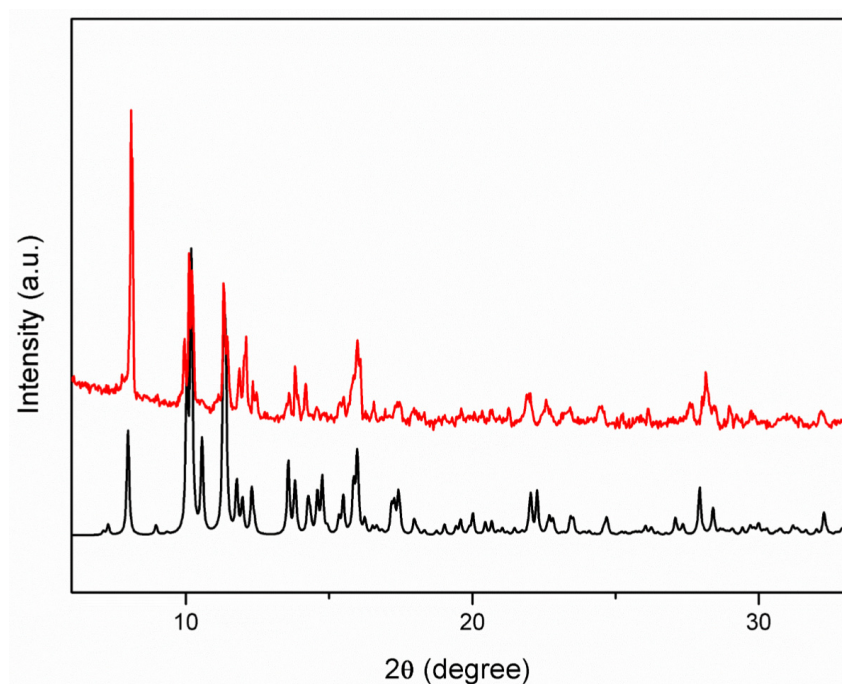
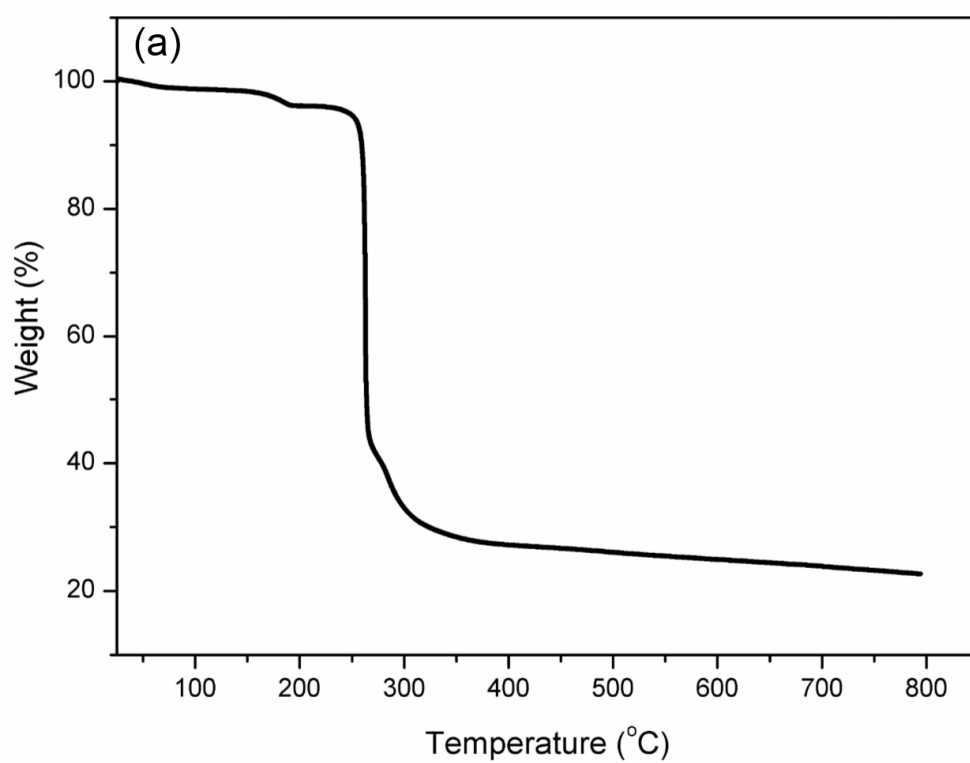
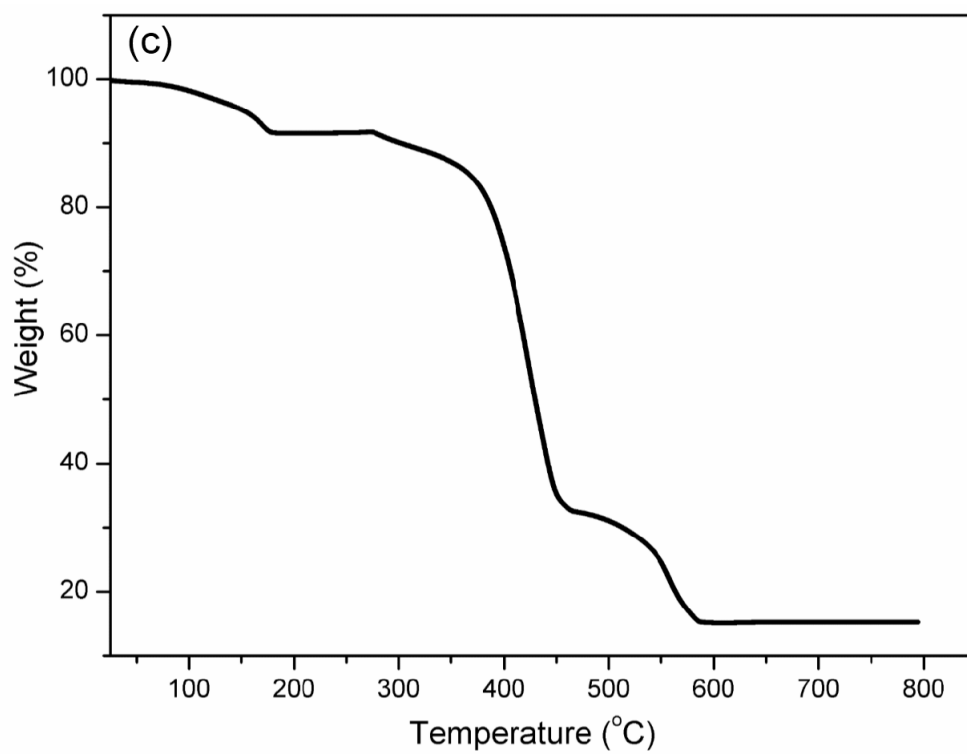
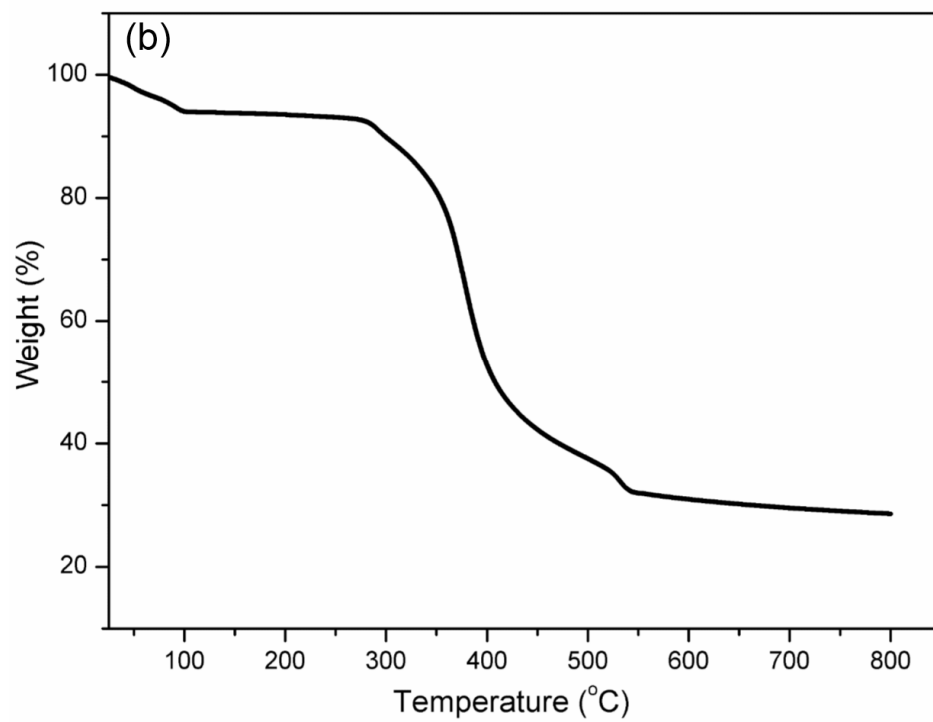


Fig. S2 PXRD pattern of compound **1** (red) and the simulated PXRD pattern (black).





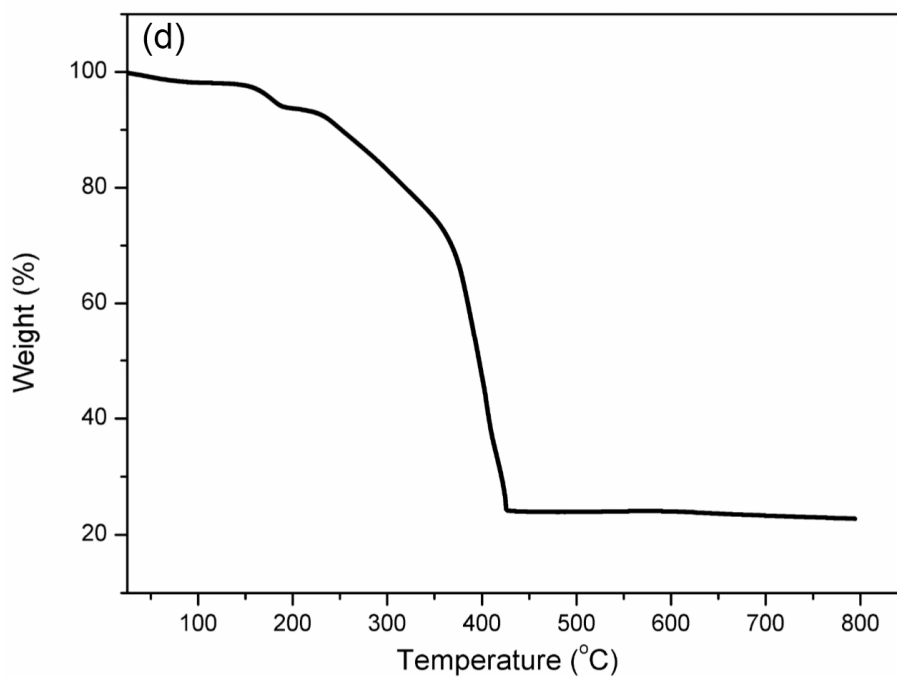
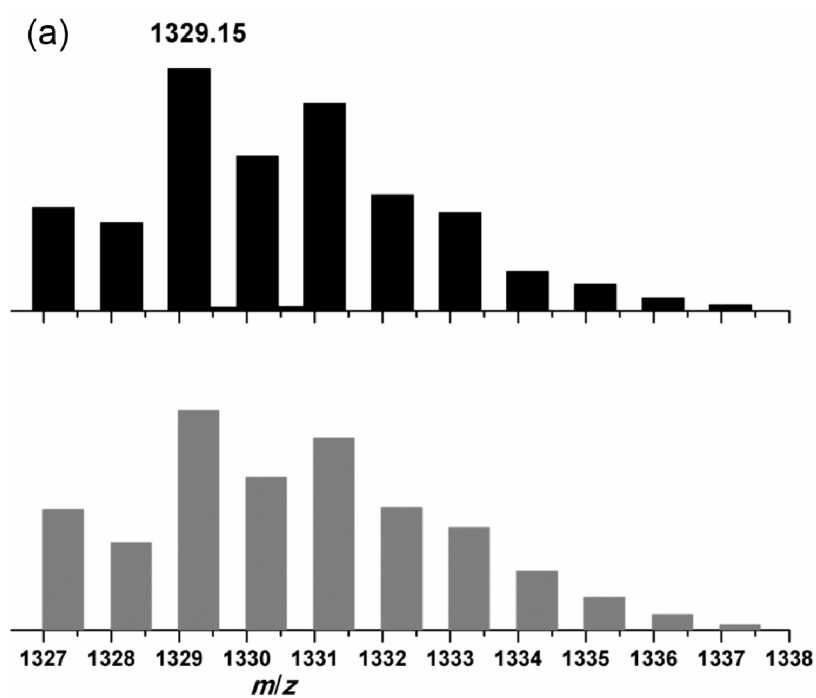
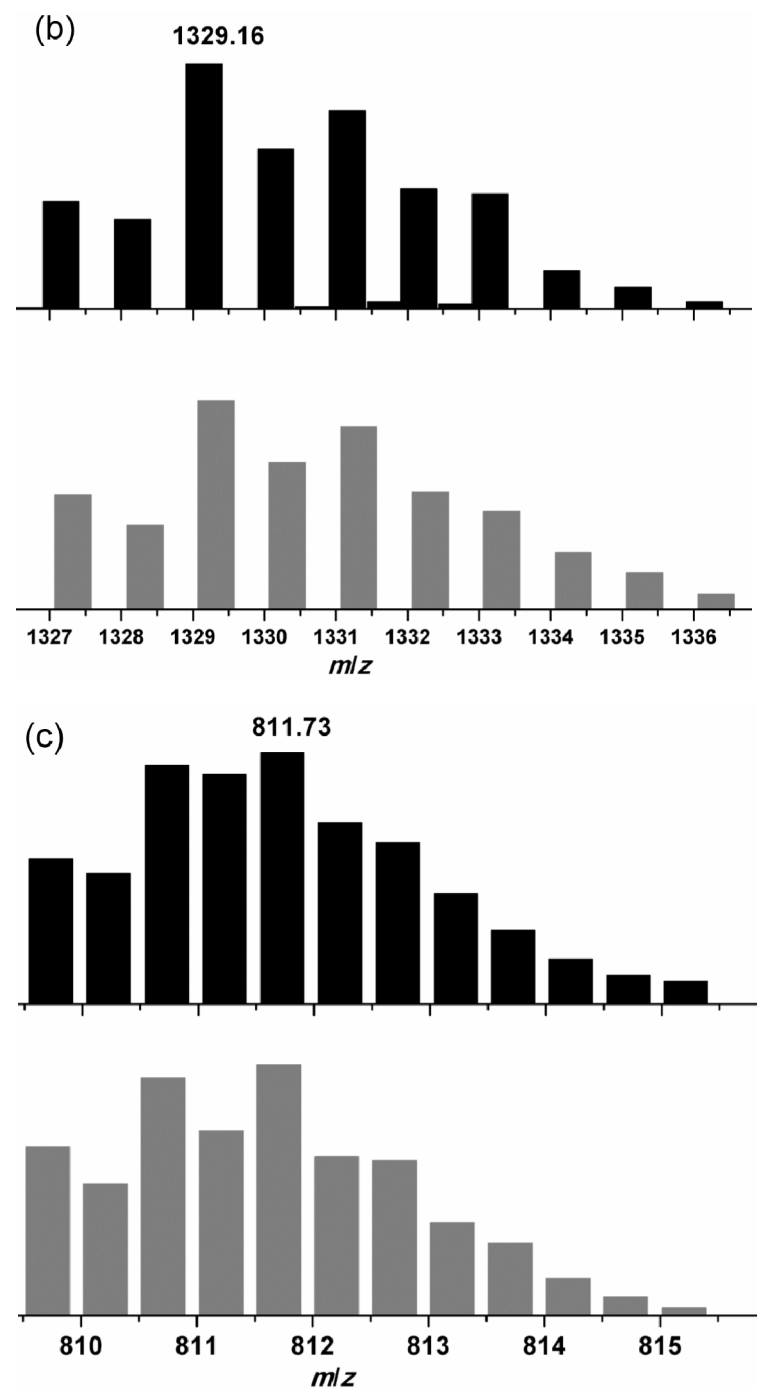


Fig. S3 TGA of compound **1** (a), **2** (b), **3** (c) and **4** (d) collected under an N₂ atmosphere.





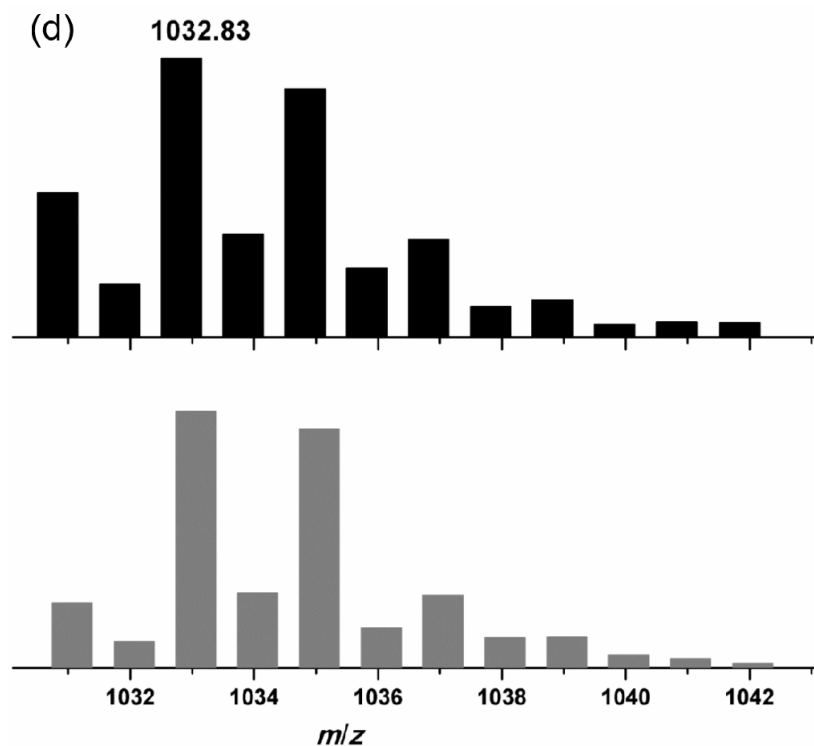


Fig. S4 The positive-ion ESI mass spectrum (black) and the calculated isotope pattern (gray) of the $[\text{Ni}_4\text{L}_4(\text{HCOO})_3]^+$ cation of **1** (a). The positive-ion ESI mass spectrum (black) and the calculated isotope pattern (gray) of the $[\text{Ni}_4\text{L}_4(\text{OAc})_2(\text{OH})]^+$ cation of **2** (b). The positive-ion ESI mass spectrum (black) and the calculated isotope pattern (gray) of the $\{[\text{Ni}_4\text{L}_4\text{Cl}_4(\text{EtOH})_5(\text{H}_2\text{O})_3] + 2\text{H}^+\}^{2+}$ cation of **3** (c). The positive-ion ESI mass spectrum (black) and the calculated isotope pattern (gray) of the $\{[\text{Ni}_2\text{L}_2\text{Br}_3(\text{MeOH})(\text{DMF})_2(\text{H}_2\text{O})] + 2\text{H}^+\}^+$ cation of **4** (d).

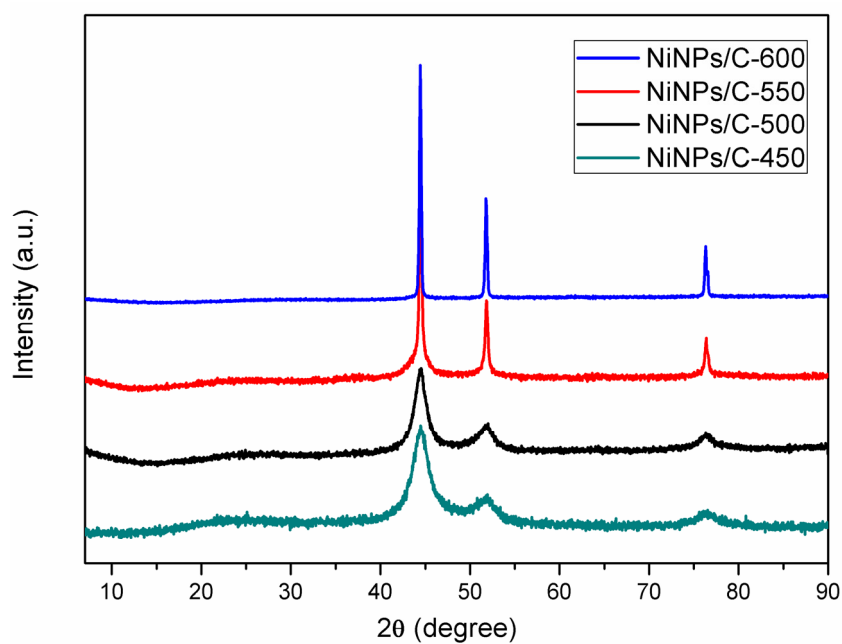


Fig. S5 PXRd patterns of NiNPs/C-450, NiNPs/C-500, NiNPs/C-550, NiNPs/C-600.

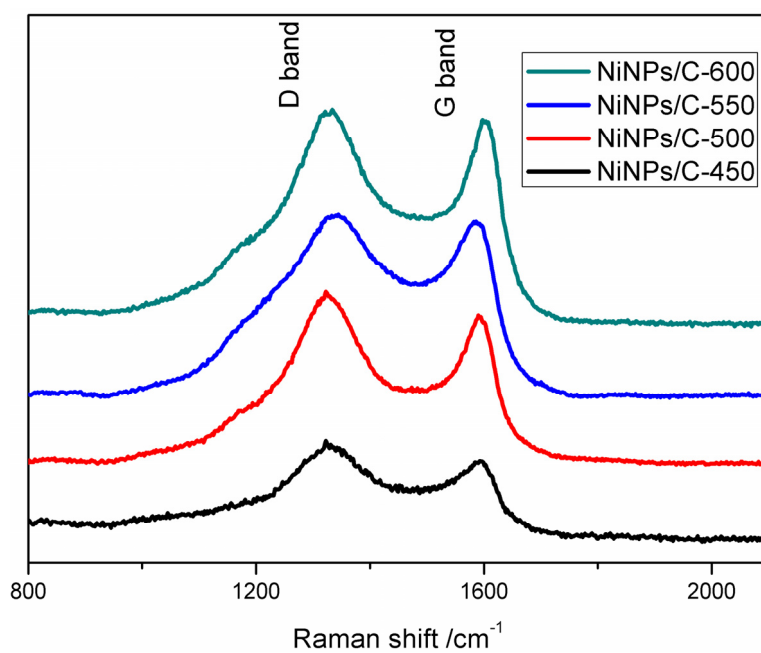


Fig. S6 Raman spectra of the obtained NiNPs/C-450, NiNPs/C-500, NiNPs/C-550, NiNPs/C-600.

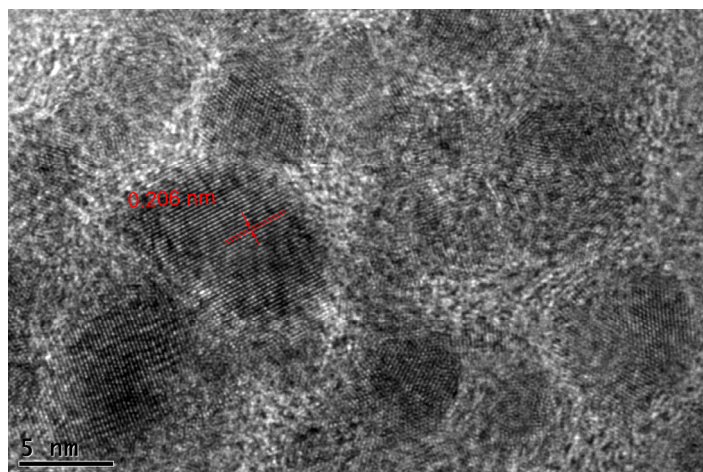
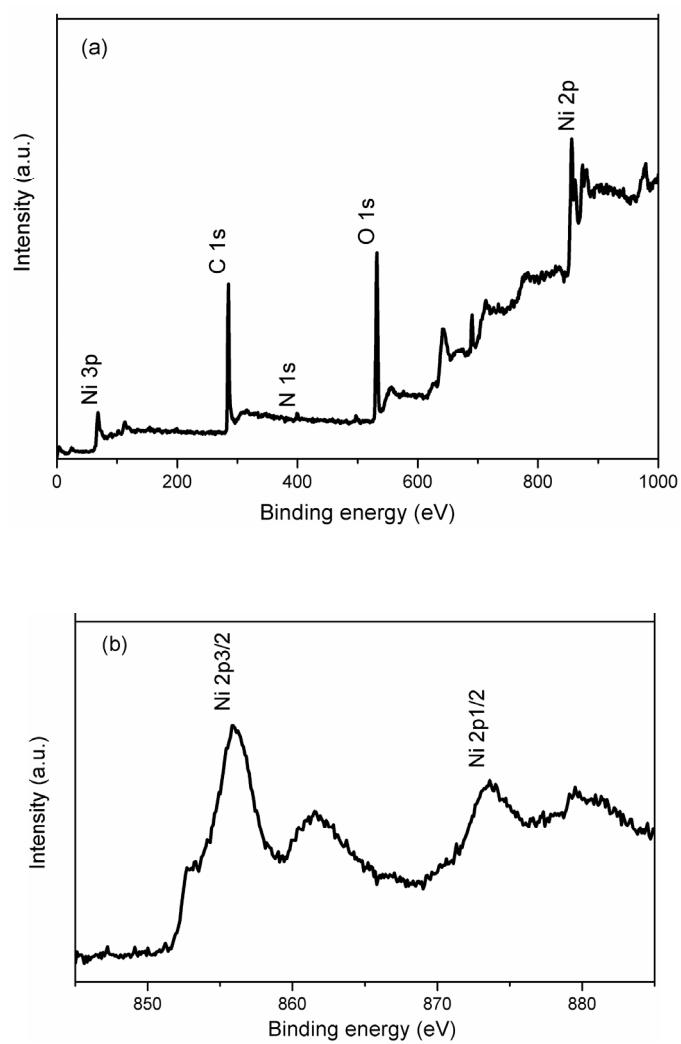


Fig. S7 HRTEM image of the obtained NiNPs/C-450.



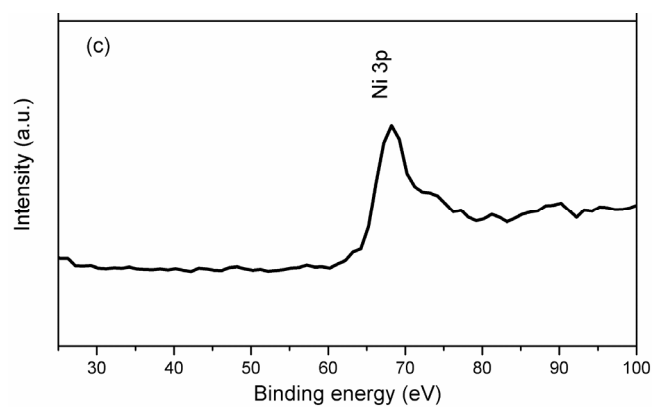


Fig. S8 XPS spectra of NiNPs/C-450 (a), Ni 2p (b), and Ni 3p (c).

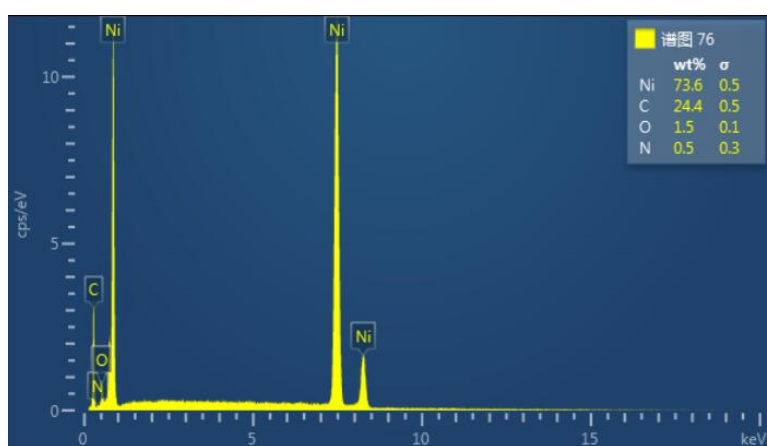


Fig. S9 The EDX spectrum of NiNPs/C-450.

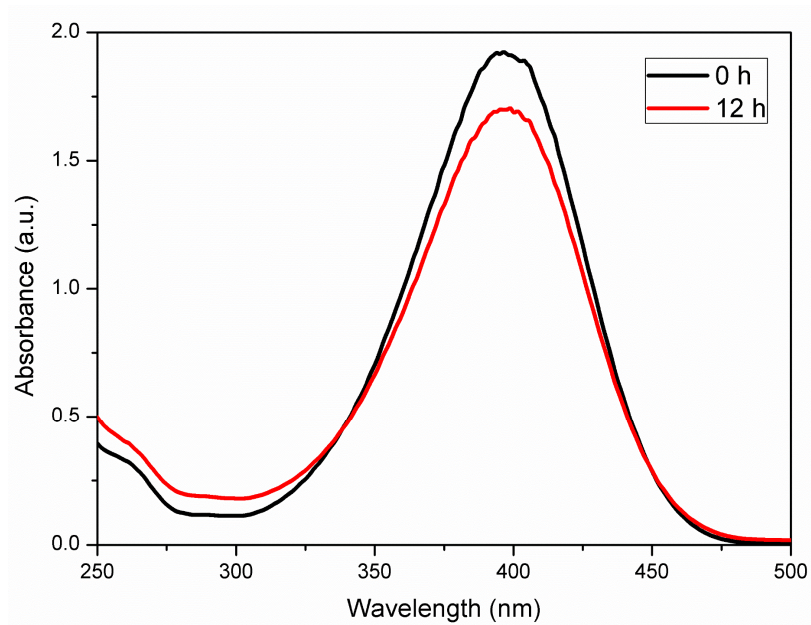


Fig. S10 UV-vis absorption spectra for the catalytic reduction of 4-NP without adding any catalysts at time zero and after 12 h.

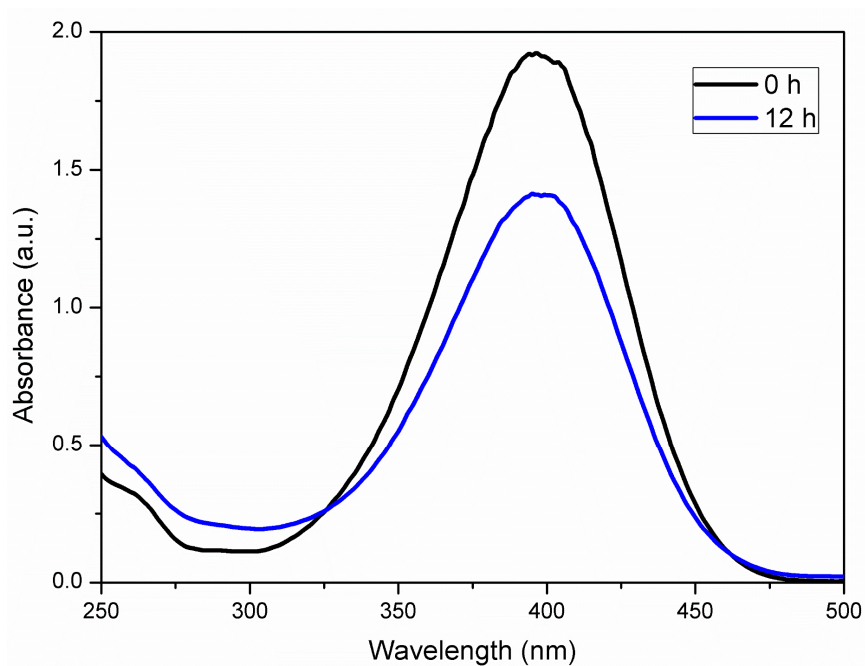


Fig. S11 UV-vis absorption spectra for the catalytic reduction of 4-NP with compound **1** as a catalyst at time zero and after 12 h.

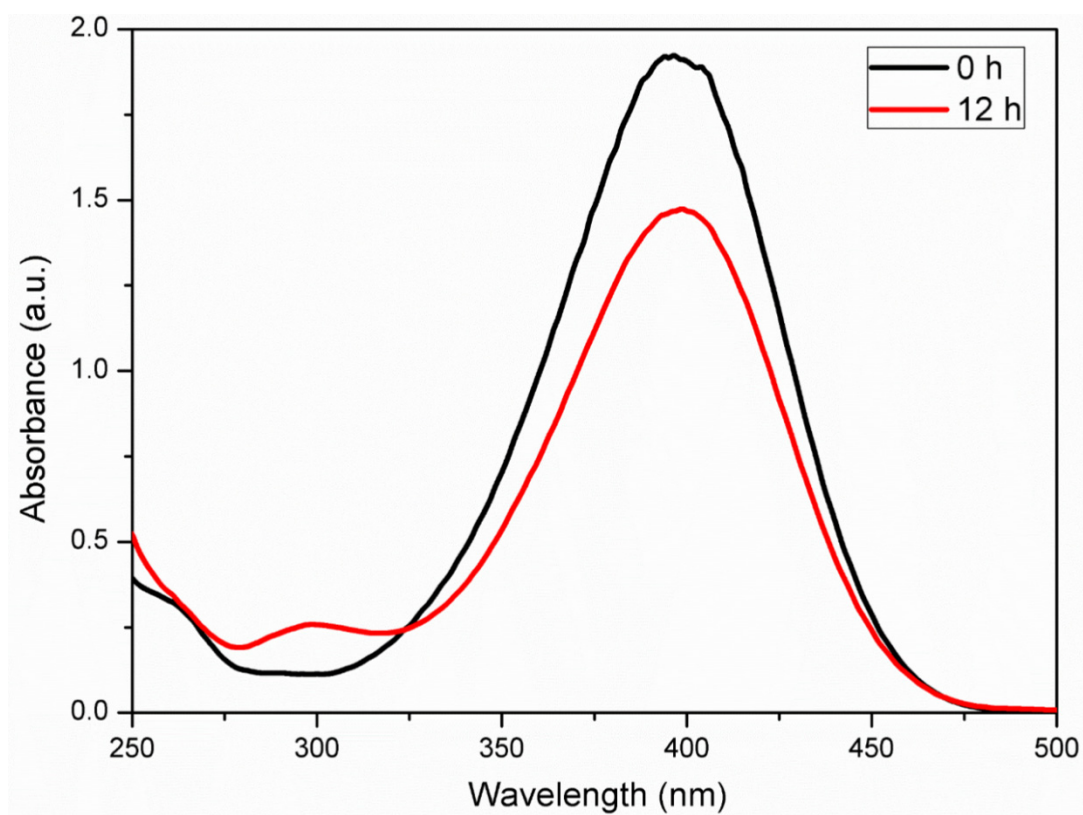


Fig. S12 UV-vis absorption spectra for the catalytic reduction of 4-NP with metal-free host material as a catalyst at time zero and after 12 h.

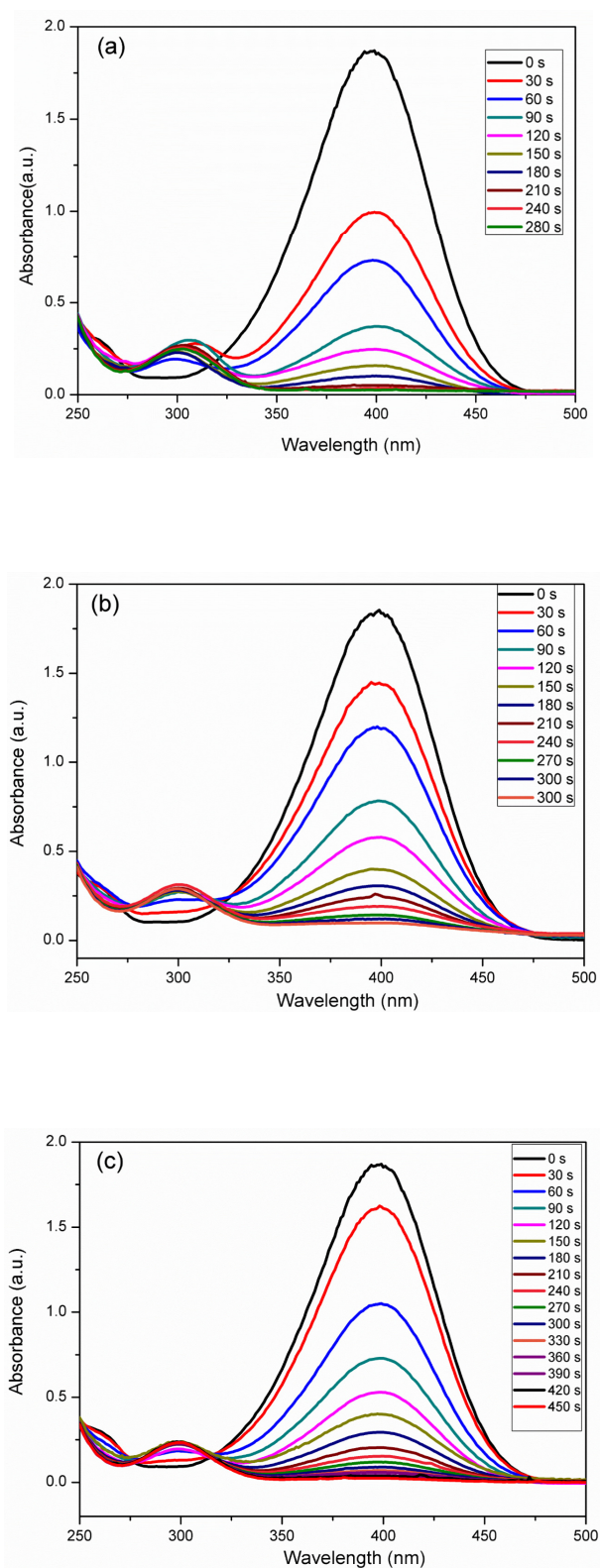


Fig. S13 UV-vis absorption spectra for the catalytic reduction of 4-NP with NiNPs/C-500 (a), NiNPs/C-550 (b), and NiNPs/C-600 (c).

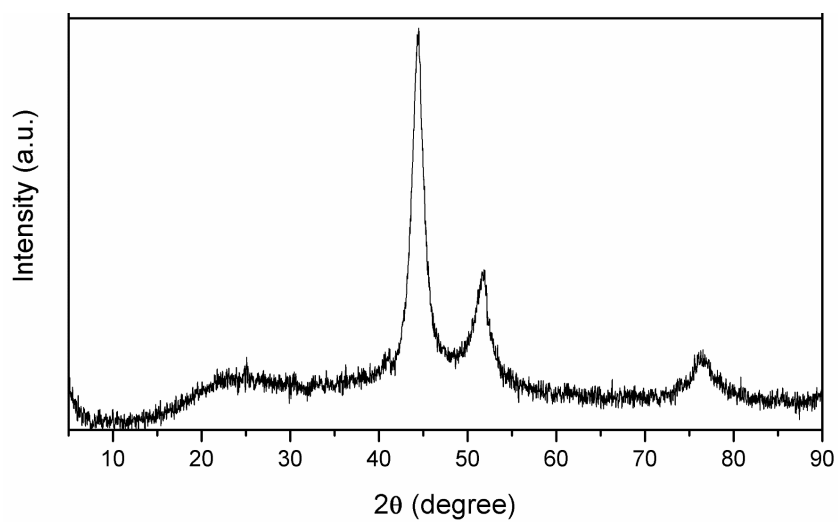
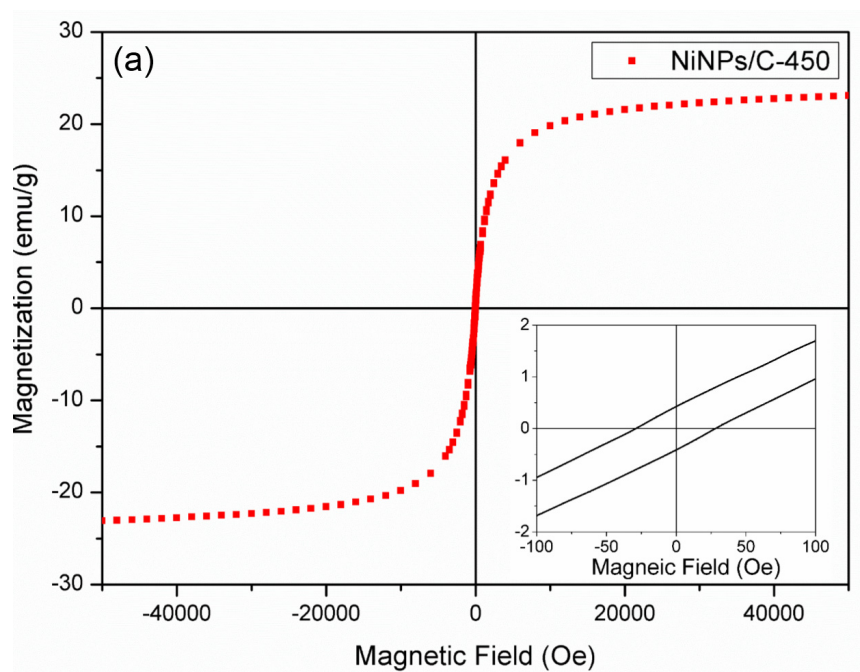


Fig. S14 PXRD spectrum of NiNPs/C-450 after 10 catalytic cycles.



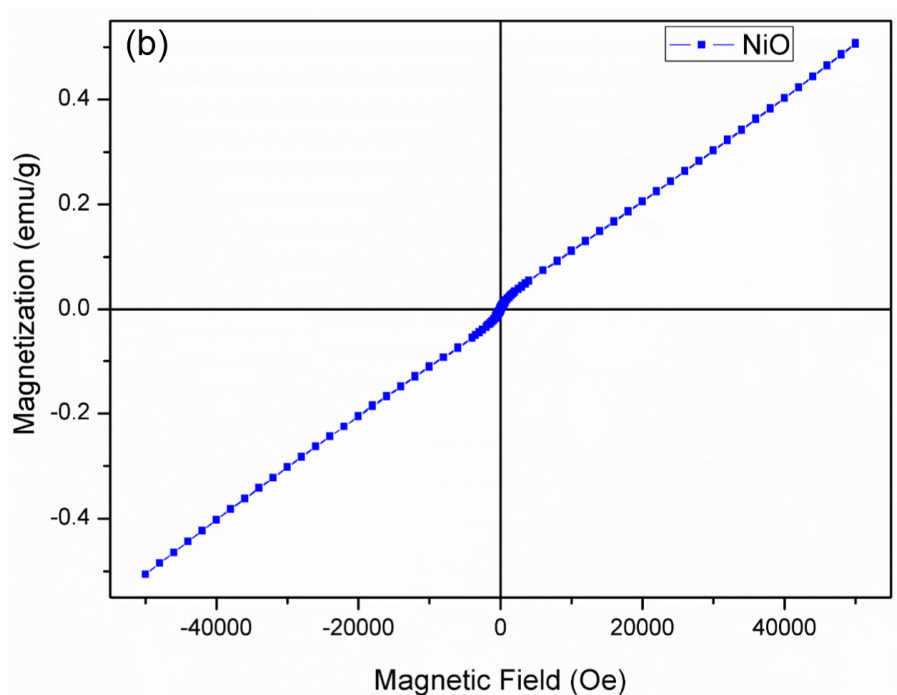


Fig. S15 The hysteresis loops obtained for NiNPs/C-450 with inset of shows the width of the hysteresis loop near the zero filed (a). The hysteresis loops obtained for NiO (b).

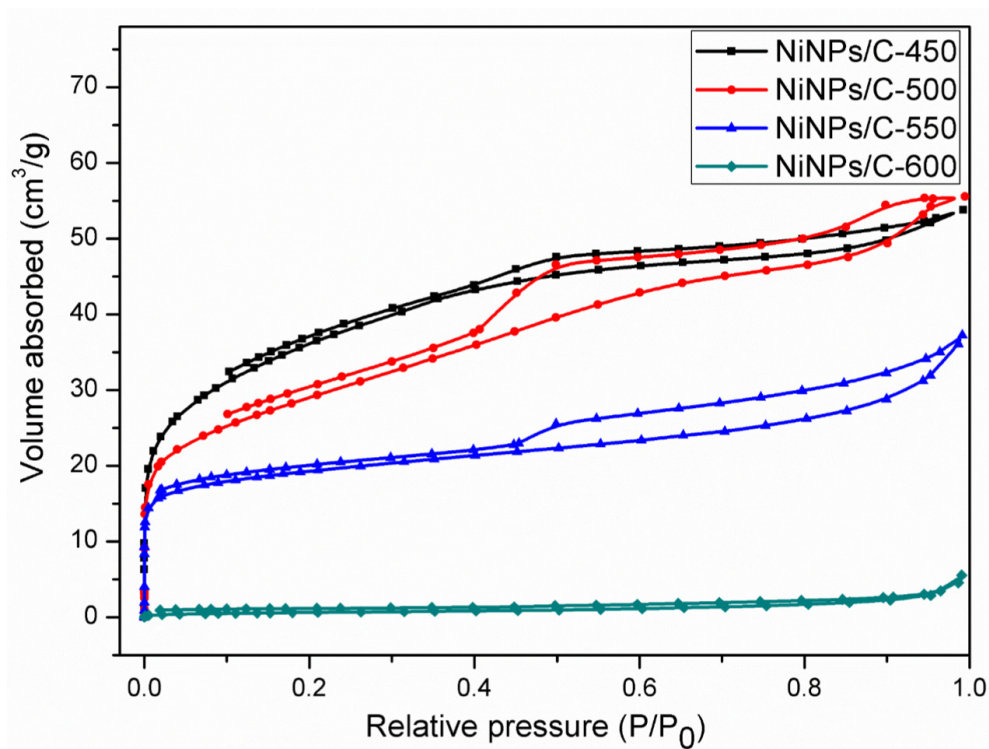


Fig. S16 N₂ adsorption-desorption isotherms of NiNPs/C-450 (black), NiNPs/C-500 (red), NiNPs/C-550 (blue) and NiNPs/C-600 (olive).

8. Tables S1 – S5

Table S1 Crystal data and structure refinement parameters for 1 – 4

Compounds	1	2	3	4
Formula	C ₆₈ H ₈₂ N ₄ Ni ₄ O ₁₅	C ₁₅₀ H ₂₀₄ N ₈ Ni ₈ O ₃₆	C ₇₂ H ₉₆ Cl ₄ N ₄ Ni ₄ O ₈	C ₆₈ H ₈₄ Br ₄ N ₄ Ni ₄ O ₈
Formula weight	1430.21	3164.88	1522.16	1639.87
Crystal system	triclinic	triclinic	monoclinic	monoclinic
Space group	<i>P</i> $\bar{1}$	<i>P</i> $\bar{1}$	<i>C</i> 2/ <i>c</i>	<i>C</i> 2/ <i>c</i>
<i>a</i> /Å	12.2603(4)	12.3023(11)	30.848(4)	27.418(3)
<i>b</i> /Å	12.8921(4)	16.2603(14)	16.941(2)	17.6175 (18)
<i>c</i> /Å	23.0008(8)	22.3585(18)	33.157(4)	30.949(3)
α /°	76.203(3)	102.451(2)	90	90
β /°	84.493(3)	100.521(2)	104.778(3)	101.688(2)
γ /°	88.665	109.527(2)	90	90
<i>V</i> /Å ³	3514.3(2)	3955.5(6)	16755(4)	14640 (2)
<i>D</i> _c /(g cm ⁻³)	1.352	1.329	1.207	1.488
<i>Z</i>	2	1	8	8
μ (Mo–K α)/mm ⁻¹	1.120	1.005	1.061	3.249
<i>F</i> (000)	1500	1672	6400	6688
Total reflections	40873	193877	248890	136657
Unique reflections	18299	19637	20796	16135
No observations	12527	14822	15044	9629
No parameters	850	956	945	837
<i>R</i> _{int}	0.0406	0.0556	0.0659	0.1101
<i>R</i> ^a	0.0624	0.0363	0.0955	0.0869
<i>wR</i> ^b	0.1638	0.0777	0.2224	0.1908
<i>GOF</i> ^c	1.071	1.021	1.106	1.065

^a*R* = $\Sigma ||F_o| - |F_c|| / \Sigma |F_o|$. ^b*wR* = $\{\Sigma w(F_o^2 - F_c^2)^2 / \Sigma w(F_o^2)^2\}^{1/2}$. ^cGOF = $\{\Sigma w((F_o^2 - F_c^2)^2) / (n - p)\}^{1/2}$, where *n* = number of reflections and *p* = total number of parameters refined.

Table S2 Selected bond lengths (Å) and angles (°) for 1 – 4

Compound 1			
Ni(1)-Ni(3)	2.9557(7)	Ni(2)-Ni(4)	2.8895(6)
Ni(1)-Ni(2)	3.1717(6)	Ni(1)-Ni(4)	3.1789(7)
Ni(2)-Ni(3)	3.1989(6)	Ni(3)-Ni(4)	3.1519(6)
Ni(1)-O(1)	2.090(2)	Ni(1)-O(2)	2.086(2)
Ni(1)-O(3)	2.043(2)	Ni(1)-O(6)	2.016(3)
Ni(1)-N(1)	2.086(3)	Ni(1)-O(8)	2.076(3)
Ni(2)-O(1W)	2.023(3)	Ni(2)-O(1)	2.058(2)
Ni(2)-O(2)	2.055(2)	Ni(2)-O(4)	2.077(3)
Ni(2)-O(11)	2.071(3)	Ni(2)-N(2)	2.066(3)
Ni(3)-O(10)	2.039(3)	Ni(3)-O(1)	2.064(3)

Ni(3)-O(7)	2.062(3)	Ni(3)-O(3)	2.080(2)
Ni(3)-N(3)	2.065(3)	Ni(3)-O(4)	2.085(2)
Ni(4)-O(2W)	2.001(3)	Ni(4)-O(2)	2.051(3)
Ni(4)-O(3)	2.050(2)	Ni(4)-O(4)	2.069(2)
Ni(4)-N(4)	2.065(3)	Ni(4)-O(12)	2.092(3)
O(6)-Ni(1)-O(3)	103.40(11)	O(3)-Ni(1)-O(8)	91.43(11)
O(6)-Ni(1)-O(8)	88.34(11)	O(3)-Ni(1)-N(1)	164.00(11)
O(6)-Ni(1)-N(1)	92.58(12)	O(6)-Ni(1)-O(2)	100.23(10)
O(8)-Ni(1)-N(1)	88.21(12)	O(8)-Ni(1)-O(2)	168.04(11)
O(3)-Ni(1)-O(2)	78.53(10)	O(6)-Ni(1)-O(1)	170.80(12)
N(1)-Ni(1)-O(2)	99.62(11)	O(8)-Ni(1)-O(1)	93.55(10)
O(3)-Ni(1)-O(1)	85.57(10)	O(2)-Ni(1)-O(1)	79.32(9)
N(1)-Ni(1)-O(1)	78.49(11)	O(1W)-Ni(2)-O(1)	91.39(10)
O(1W)-Ni(2)-O(2)	170.05(12)	O(1W)-Ni(2)-N(2)	96.19(12)
O(2)-Ni(2)-O(1)	80.80(9)	O(1)-Ni(2)-N(2)	100.87(11)
O(2)-Ni(2)-N(2)	79.40(11)	O(2)-Ni(2)-O(11)	95.90(10)
O(1W)-Ni(2)-O(11)	92.89(11)	N(2)-Ni(2)-O(11)	88.61(12)
O(1)-Ni(2)-O(11)	169.12(11)	O(2)-Ni(2)-O(4)	88.09(9)
O(1W)-Ni(2)-O(4)	96.51(11)	N(2)-Ni(2)-O(4)	167.30(11)
O(1)-Ni(2)-O(4)	79.04(10)	O(11)-Ni(2)-O(4)	90.53(11)
O(10)-Ni(3)-O(7)	89.47(12)	O(7)-Ni(3)-O(1)	92.04(11)
O(10)-Ni(3)-O(1)	105.27(11)	O(7)-Ni(3)-N(3)	86.13(13)
O(10)-Ni(3)-N(3)	89.97(12)	O(10)-Ni(3)-O(3)	168.49(12)
O(1)-Ni(3)-N(3)	164.65(11)	O(1)-Ni(3)-O(3)	85.30(9)
O(7)-Ni(3)-O(3)	94.77(10)	O(10)-Ni(3)-O(4)	97.08(11)
N(3)-Ni(3)-O(3)	79.67(11)	O(7)-Ni(3)-O(4)	169.80(11)
O(1)-Ni(3)-O(4)	78.72(10)	N(3)-Ni(3)-O(4)	101.63(12)
O(3)-Ni(3)-O(4)	80.30(9)	N(4)-Ni(4)-O(12)	89.03(12)
O(2W)-Ni(4)-O(3)	93.79(11)	O(3)-Ni(4)-O(2)	79.17(9)
O(2W)-Ni(4)-O(2)	94.63(12)	O(3)-Ni(4)-N(4)	98.88(11)
O(2W)-Ni(4)-N(4)	97.57(13)	O(2W)-Ni(4)-O(4)	173.72(12)
O(2)-Ni(4)-N(4)	167.75(11)	O(2)-Ni(4)-O(4)	88.40(9)
O(3)-Ni(4)-O(4)	81.35(9)	O(2W)-Ni(4)-O(12)	92.04(12)
N(4)-Ni(4)-O(4)	79.36(11)	O(2)-Ni(4)-O(12)	91.62(11)
O(3)-Ni(4)-O(12)	169.46(10)	O(4)-Ni(4)-O(12)	93.38(10)
Compound 2			
Ni(1)-Ni(3)	3.1987(4)	Ni(2)-Ni(4)	3.2081(4)
Ni(1)-Ni(2)	2.9251(4)	Ni(1)-Ni(4)	3.1538(5)

Ni(2)-Ni(3)	3.0959(4)	Ni(3)-Ni(4)	2.9384(4)
Ni(1)-O(6)	2.0178(14)	Ni(1)-N(1)	2.0727(16)
Ni(1)-O(4)	2.0653(14)	Ni(1)-O(1)	2.0797(13)
Ni(1)-O(7)	2.0729(15)	Ni(1)-O(2)	2.0352(13)
Ni(2)-O(2)	2.0379(13)	Ni(2)-O(13)	2.0450(14)
Ni(2)-O(8)	2.0409(15)	Ni(2)-O(1)	2.0674(13)
Ni(2)-O(3)	2.0619(14)	Ni(2)-N(2)	2.0864(16)
Ni(3)-O(1W)	2.0083(15)	Ni(3)-O(3)	2.0595(13)
Ni(3)-O(4)	2.0441(13)	Ni(3)-O(12)	2.0736(15)
Ni(3)-N(3)	2.0687(16)	Ni(3)-O(2)	2.0778(14)
Ni(4)-O(4)	2.0820(13)	Ni(4)-O(11)	2.0489(15)
Ni(4)-O(9)	2.0280(14)	Ni(4)-O(3)	2.0786(13)
Ni(4)-N(4)	2.0899(16)	Ni(4)-O(1)	2.0616(14)
O(6)-Ni(1)-O(4)	103.19(6)	O(7)-Ni(1)-O(1)	91.00(5)
O(6)-Ni(1)-O(2)	103.52(6)	O(6)-Ni(1)-N(1)	91.15(6)
O(2)-Ni(1)-O(4)	78.07(5)	O(4)-Ni(1)-N(1)	101.79(6)
O(2)-Ni(1)-N(1)	165.02(6)	O(2)-Ni(1)-O(7)	91.04(6)
O(6)-Ni(1)-O(7)	86.84(6)	N(1)-Ni(1)-O(7)	86.70(6)
O(4)-Ni(1)-O(7)	166.58(5)	O(2)-Ni(1)-O(1)	86.27(5)
O(6)-Ni(1)-O(1)	170.00(6)	N(1)-Ni(1)-O(1)	78.98(6)
O(4)-Ni(1)-O(1)	80.59(5)	O(2)-Ni(2)-O(8)	95.78(6)
O(2)-Ni(2)-O(13)	170.48(6)	O(8)-Ni(2)-O(13)	93.29(6)
O(2)-Ni(2)-O(3)	82.70(5)	O(8)-Ni(2)-O(3)	169.12(5)
O(13)-Ni(2)-O(3)	88.93(6)	O(2)-Ni(2)-O(1)	86.52(5)
O(8)-Ni(2)-O(1)	90.83(6)	O(13)-Ni(2)-O(1)	96.26(5)
O(3)-Ni(2)-O(1)	78.33(5)	O(2)-Ni(2)-N(2)	79.29(6)
O(8)-Ni(2)-N(2)	86.71(6)	O(13)-Ni(2)-N(2)	98.37(6)
O(3)-Ni(2)-N(2)	103.52(6)	O(1)-Ni(2)-N(2)	165.27(6)
O(1W)-Ni(3)-O(4)	93.61(6)	O(1W)-Ni(3)-O(3)	172.61(7)
O(4)-Ni(3)-O(3)	87.18(5)	O(1W)-Ni(3)-N(3)	99.23(7)
O(4)-Ni(3)-N(3)	167.08(6)	O(3)-Ni(3)-N(3)	79.91(6)
O(1W)-Ni(3)-O(12)	95.43(7)	O(4)-Ni(3)-O(12)	91.92(6)
O(3)-Ni(3)-O(12)	91.88(6)	N(3)-Ni(3)-O(12)	88.27(6)
O(1W)-Ni(3)-O(2)	91.20(6)	O(4)-Ni(3)-O(2)	77.59(5)
O(3)-Ni(3)-O(2)	81.79(5)	N(3)-Ni(3)-O(2)	100.63(6)
O(12)-Ni(3)-O(2)	167.94(5)	O(9)-Ni(4)-O(11)	91.66(6)
O(9)-Ni(4)-O(1)	96.06(6)	O(11)-Ni(4)-O(1)	168.07(5)
O(9)-Ni(4)-O(3)	106.92(5)	O(11)-Ni(4)-O(3)	90.99(6)

O(1)-Ni(4)-O(3)	78.08(5)	O(9)-Ni(4)-O(4)	166.13(6)
O(11)-Ni(4)-O(4)	93.93(6)	O(1)-Ni(4)-O(4)	80.63(5)
O(3)-Ni(4)-O(4)	85.69(5)	O(9)-Ni(4)-N(4)	89.68(6)
O(11)-Ni(4)-N(4)	90.18(6)	O(1)-Ni(4)-N(4)	98.92(6)
O(3)-Ni(4)-N(4)	163.32(6)	O(4)-Ni(4)-N(4)	77.63(6)
Compound 3			
Ni(1)-Ni(3)	3.0804(11)	Ni(2)-Ni(4)	3.1104(11)
Ni(1)-Ni(2)	3.1803(12)	Ni(1)-Ni(4)	3.0965(10)
Ni(2)-Ni(3)	3.0832(11)	Ni(3)-Ni(4)	3.1818(11)
Ni(1)-N(1)	2.037(5)	Ni(1)-O(5)	2.091(5)
Ni(1)-O(3)	2.049(3)	Ni(1)-Cl(1)	2.3492(15)
Ni(1)-O(1)	2.063(4)	Ni(1)-O(2)	2.107(4)
Ni(2)-N(2)	2.054(5)	Ni(2)-O(6)	2.110(5)
Ni(2)-O(2)	2.053(4)	Ni(2)-Cl(2)	2.3623(18)
Ni(2)-O(4)	2.057(4)	Ni(2)-O(1)	2.116(5)
Ni(3)-N(3)	2.043(4)	Ni(3)-O(4)	2.087(4)
Ni(3)-O(2)	2.039(3)	Ni(3)-Cl(3)	2.3729(17)
Ni(3)-O(3)	2.054(4)	Ni(3)-O(7)	2.089(4)
Ni(4)-O(1)	2.058(4)	Ni(4)-O(3)	2.099(4)
Ni(4)-N(4)	2.056(5)	Ni(4)-Cl(4)	2.3588(18)
Ni(4)-O(4)	2.066(4)	Ni(4)-O(8)	2.107(5)
N(1)-Ni(1)-O(1)	79.81(18)	N(1)-Ni(1)-O(5)	89.2(2)
N(1)-Ni(1)-O(3)	162.28(18)	O(1)-Ni(1)-O(5)	90.95(19)
O(3)-Ni(1)-O(1)	82.70(15)	O(3)-Ni(1)-O(2)	81.71(14)
O(3)-Ni(1)-O(5)	88.28(17)	O(5)-Ni(1)-O(2)	167.47(16)
N(1)-Ni(1)-O(2)	98.08(18)	O(3)-Ni(1)-Cl(1)	100.19(11)
O(1)-Ni(1)-O(2)	80.36(17)	O(5)-Ni(1)-Cl(1)	92.98(14)
N(1)-Ni(1)-Cl(1)	97.46(15)	O(1)-Ni(1)-Cl(1)	175.18(12)
O(2)-Ni(1)-Cl(1)	96.18(11)	O(2)-Ni(2)-N(2)	79.61(16)
N(2)-Ni(2)-O(4)	161.20(18)	N(2)-Ni(2)-O(6)	86.4(2)
O(2)-Ni(2)-O(4)	82.38(15)	O(2)-Ni(2)-O(1)	80.38(16)
O(2)-Ni(2)-O(6)	91.99(17)	O(4)-Ni(2)-O(1)	81.40(16)
O(4)-Ni(2)-O(6)	88.93(18)	O(2)-Ni(2)-Cl(2)	175.01(14)
N(2)-Ni(2)-O(1)	100.7(2)	O(4)-Ni(2)-Cl(2)	100.17(13)
O(6)-Ni(2)-O(1)	168.36(17)	O(1)-Ni(2)-Cl(2)	95.70(12)
N(2)-Ni(2)-Cl(2)	98.20(14)	O(6)-Ni(2)-Cl(2)	92.35(14)
O(2)-Ni(3)-O(3)	83.26(15)	O(2)-Ni(3)-O(4)	81.99(15)
O(2)-Ni(3)-N(3)	162.18(17)	O(3)-Ni(3)-O(4)	80.06(16)

N(3)-Ni(3)-O(3)	79.91(16)	N(3)-Ni(3)-O(7)	88.95(18)
N(3)-Ni(3)-O(4)	100.71(17)	O(4)-Ni(3)-O(7)	167.06(17)
O(2)-Ni(3)-O(7)	86.21(16)	N(3)-Ni(3)-Cl(3)	96.95(14)
O(3)-Ni(3)-O(7)	93.33(16)	O(4)-Ni(3)-Cl(3)	95.60(13)
O(2)-Ni(3)-Cl(3)	100.33(12)	O(3)-Ni(3)-Cl(3)	173.99(11)
O(7)-Ni(3)-Cl(3)	91.72(13)	N(4)-Ni(4)-O(1)	162.1(2)
O(1)-Ni(4)-O(4)	82.59(17)	O(1)-Ni(4)-O(3)	81.63(14)
N(4)-Ni(4)-O(4)	80.34(17)	N(4)-Ni(4)-O(8)	86.7(2)
N(4)-Ni(4)-O(3)	100.28(17)	O(4)-Ni(4)-O(8)	91.3(2)
O(4)-Ni(4)-O(3)	79.53(16)	N(4)-Ni(4)-Cl(4)	96.83(14)
O(1)-Ni(4)-O(8)	88.56(18)	O(4)-Ni(4)-Cl(4)	174.40(13)
O(3)-Ni(4)-O(8)	167.33(17)	O(8)-Ni(4)-Cl(4)	93.34(18)
O(1)-Ni(4)-Cl(4)	100.62(14)	O(3)-Ni(4)-Cl(4)	96.32(12)
Compound 4			
Ni(1)-Ni(3)	3.1628(16)	Ni(2)-Ni(4)	3.150(2)
Ni(1)-Ni(2)	3.1238(17)	Ni(1)-Ni(4)	3.1196(19)
Ni(2)-Ni(3)	3.1081(15)	Ni(3)-Ni(4)	3.1048(17)
Ni(1)-O(4)	2.041(6)	Ni(1)-O(5)	2.105(11)
Ni(1)-O(1)	2.045(7)	Ni(1)-Br(1)	2.506(2)
Ni(1)-N(1)	2.073(9)	Ni(1)-O(3)	2.119(7)
Ni(2)-O(1)	2.052(5)	Ni(2)-O(4)	2.106(8)
Ni(2)-N(2)	2.045(6)	Ni(2)-Br(2)	2.5061(16)
Ni(2)-O(2)	2.055(6)	Ni(2)-O(6)	2.124(9)
Ni(3)-O(7)	2.093(6)	Ni(3)-N(3)	2.071(6)
Ni(3)-O(3)	2.037(7)	Ni(3)-Br(3)	2.5133(16)
Ni(3)-O(2)	2.071(5)	Ni(3)-O(1)	2.105(6)
Ni(4)-O(3)	2.050(6)	Ni(4)-O(2)	2.077(6)
Ni(4)-O(4)	2.050(7)	Ni(4)-Br(4)	2.5325(18)
Ni(4)-N(4)	2.059(7)	Ni(4)-O(8)	2.087(10)
O(4)-Ni(1)-N(1)	160.4(4)	O(4)-Ni(1)-O(5)	88.5(3)
O(4)-Ni(1)-O(1)	81.6(3)	N(1)-Ni(1)-O(5)	87.2(4)
O(1)-Ni(1)-N(1)	79.4(4)	O(1)-Ni(1)-O(3)	80.1(3)
O(1)-Ni(1)-O(5)	91.6(5)	O(5)-Ni(1)-O(3)	167.0(3)
O(4)-Ni(1)-O(3)	80.4(2)	O(1)-Ni(1)-Br(1)	174.90(17)
N(1)-Ni(1)-O(3)	101.0(3)	O(5)-Ni(1)-Br(1)	92.9(4)
O(4)-Ni(1)-Br(1)	100.8(2)	O(3)-Ni(1)-Br(1)	95.8(2)
N(1)-Ni(1)-Br(1)	98.5(3)	O(1)-Ni(2)-O(2)	82.7(2)
N(2)-Ni(2)-O(1)	161.8(3)	O(1)-Ni(2)-O(4)	79.9(3)

N(2)-Ni(2)-O(2)	80.5(2)	N(2)-Ni(2)-O(6)	83.4(3)
N(2)-Ni(2)-O(4)	104.0(3)	O(2)-Ni(2)-O(6)	91.2(3)
O(2)-Ni(2)-O(4)	80.2(2)	N(2)-Ni(2)-Br(2)	96.78(19)
O(1)-Ni(2)-O(6)	90.0(3)	O(2)-Ni(2)-Br(2)	174.92(18)
O(4)-Ni(2)-O(6)	167.4(2)	O(6)-Ni(2)-Br(2)	92.8(2)
O(1)-Ni(2)-Br(2)	100.47(18)	O(4)-Ni(2)-Br(2)	96.37(19)
O(3)-Ni(3)-O(2)	81.7(2)	O(3)-Ni(3)-O(7)	91.5(3)
O(3)-Ni(3)-N(3)	79.8(3)	O(2)-Ni(3)-O(7)	88.5(2)
N(3)-Ni(3)-O(2)	160.4(3)	N(3)-Ni(3)-O(1)	102.2(2)
N(3)-Ni(3)-O(7)	85.6(3)	O(7)-Ni(3)-O(1)	167.6(3)
O(3)-Ni(3)-O(1)	80.6(3)	N(3)-Ni(3)-Br(3)	97.3(2)
O(2)-Ni(3)-O(1)	81.0(2)	O(7)-Ni(3)-Br(3)	92.57(18)
O(3)-Ni(3)-Br(3)	174.89(19)	O(2)-Ni(3)-Br(3)	101.56(17)
O(1)-Ni(3)-Br(3)	95.9(2)	O(4)-Ni(4)-O(3)	81.8(2)
O(4)-Ni(4)-N(4)	80.5(3)	O(3)-Ni(4)-N(4)	161.8(3)
O(4)-Ni(4)-O(2)	81.0(3)	O(3)-Ni(4)-O(2)	81.2(2)
N(4)-Ni(4)-O(2)	100.0(3)	O(4)-Ni(4)-O(8)	94.1(4)
O(3)-Ni(4)-O(8)	87.0(3)	N(4)-Ni(4)-O(8)	90.2(3)
O(2)-Ni(4)-O(8)	167.7(3)	O(4)-Ni(4)-Br(4)	174.51(17)
O(3)-Ni(4)-Br(4)	102.02(19)	N(4)-Ni(4)-Br(4)	95.9(3)
O(2)-Ni(4)-Br(4)	95.64(16)	O(8)-Ni(4)-Br(4)	90.1(4)

Table S3 Hydrogen bonding parameters for 1 – 4

D-H...A	D-H (Å)	H...A (Å)	D...A (Å)	∠D-H...A (°)
Compound 1				
O1W-H1W1...O9	0.832(18)	1.76(2)	2.585(4)	70(4)
O1W-H2W1...O11#1	0.836(18)	1.93(2)	2.729(4)	159(4)
O2W-H1W2...O5	0.829(19)	1.762(19)	2.590(5)	175(5)
O2W-H2W2...O12#2	0.832(19)	1.90(2)	2.721(4)	172(5)
O3W-H1W3...O8	0.857(19)	2.03(3)	2.837(5)	157(6)
O3W-H2W3...O9	0.849(19)	1.92(2)	2.766(5)	176(6)
Symmetry codes for generating equivalent atoms: #1 -x + 1, -y, -z; #2 -x, -y, -z; #3 -x + 1, -y + 1, -z.				
Compound 2				
O1W-H1W1...O5	0.813(17)	1.836(17)	2.647(2)	174(3)
O2W-H1W2...O15	0.903(17)	1.863(17)	2.765(3)	176(3)
O13-H1O3...O10	0.814(16)	1.786(16)	2.597(2)	175(3)
O14-H1O4...O2W	0.883(18)	1.90(2)	2.770(3)	166(4)
O15-H1O5...O10	0.875(18)	1.854(19)	2.725(3)	173(4)

O2W-H2W2...O6#1	0.849(17)	2.52(3)	3.121(3)	129(3)
O2W-H2W2...O7#1	0.849(17)	2.21(2)	2.996(2)	153(3)
O1W-H2W1...O3W#2	0.864(17)	1.835(18)	2.664(2)	160(3)
O3W-H2W3...O5	0.834(17)	1.878(17)	2.710(2)	176(3)

Symmetry codes for generating equivalent atoms: #1 $x + 1, y, z$; #2 $-x + 1, -y + 1, -z$; #3 $x + 1, y - 1, z$.

Compound 3				
O5-H1O5...Cl4	0.833(4)	2.2510(16)	3.047(5)	160.2(3)
O6-H1O6...Cl3	0.839(5)	2.2432(17)	3.046(5)	160.4(3)
O7-H1O7...Cl1	0.841(4)	2.2059(14)	3.017(4)	162.0(3)
O8-H1O8...Cl2	0.853(6)	2.3204(18)	3.042(5)	142.5(4)
Compound 4				
O6-H1O6...Br3	0.82(2)	2.32(3)	3.135(6)	172(11)
O7-H1O7...Br4	0.83(2)	2.41(4)	3.190(6)	157(9)
O5-H1O5...Br2	0.82(2)	2.36(7)	3.151(11)	162(20)
O8-H1O8...Br1	0.83(2)	2.34(3)	3.157(12)	174(17)

Table S4 Comparison of different catalysts with NiNPs/C-450 for the reduction of 4-nitrophenol to 4-aminophenol

Sample	Type	k ($\times 10^{-3} \text{ s}^{-1}$)	κ ($\times 10^{-3} \text{ mg}^{-1} \cdot \text{s}^{-1}$)	Converse (%)	Reference
Fe ₃ O ₄ @SiO ₂ -Au@mSiO ₂	microsphere	5.8	1.93	90(8)	6
Ni/SiO ₂ @Au	microsphere	10	2.5	73(8)	7
p(AMPS)-Ni	hydrogel	0.9	0.15	75(5)	8
Au@C	nanocomposite	3.6	1.8	32(10)	9
Ni(modified)	nanoparticles	2.4	0.80	/	10
NiNPs/C-450	nanocomposite	19	9.5	97(10)	this work

Table S5 The BET surface area, total pore volume, and average pore size of NiNPs/C-450, NiNPs/C-500, NiNPs/C-550, NiNPs/C-600.

Sample	BET surface area ($\text{m}^2 \cdot \text{g}^{-1}$)	Pore volume ($\text{cm}^3 \cdot \text{g}^{-1}$)	Average size (nm)
NiNPs/C-450	125	0.08	2.65
NiNPs/C-500	101	0.08	3.40
NiNPs/C-550	52	0.06	4.40
NiNPs/C-600	2	0.01	14.96

9. Original ^1H NMR, ^{13}C NMR, TOF-Mass, ESI-Mass and IR spectra of HL and compounds 1 – 4.

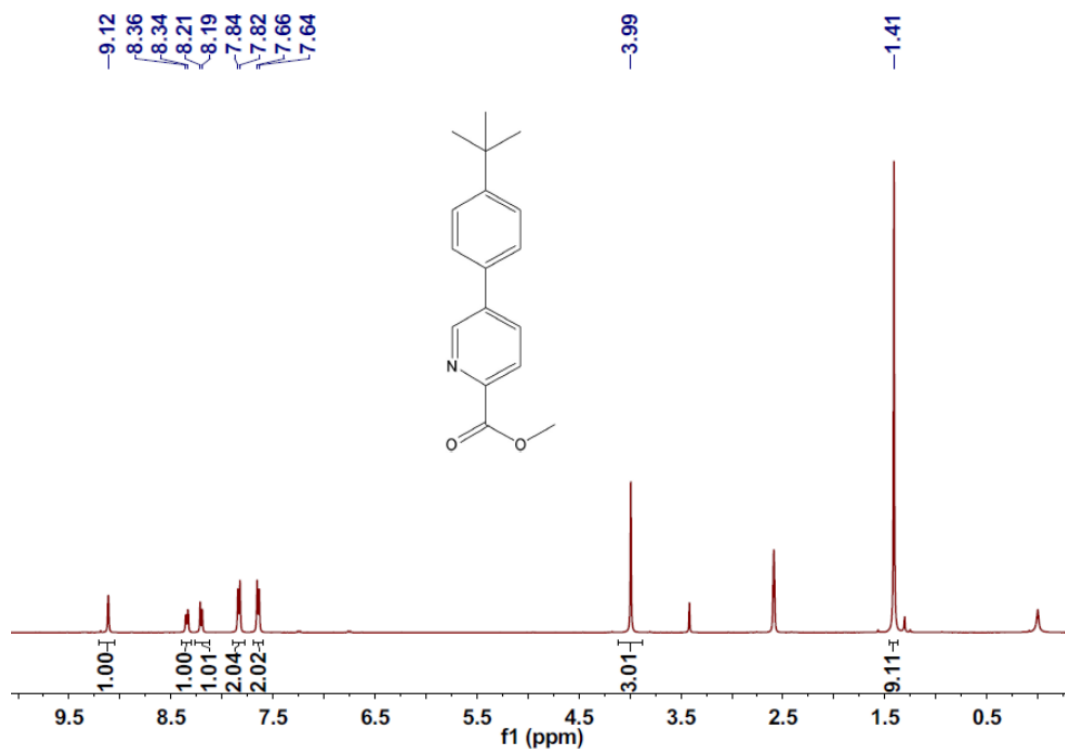


Fig. S17 The ^1H NMR spectrum of methyl 5-(4-(tert-butyl)phenyl)picolinate.

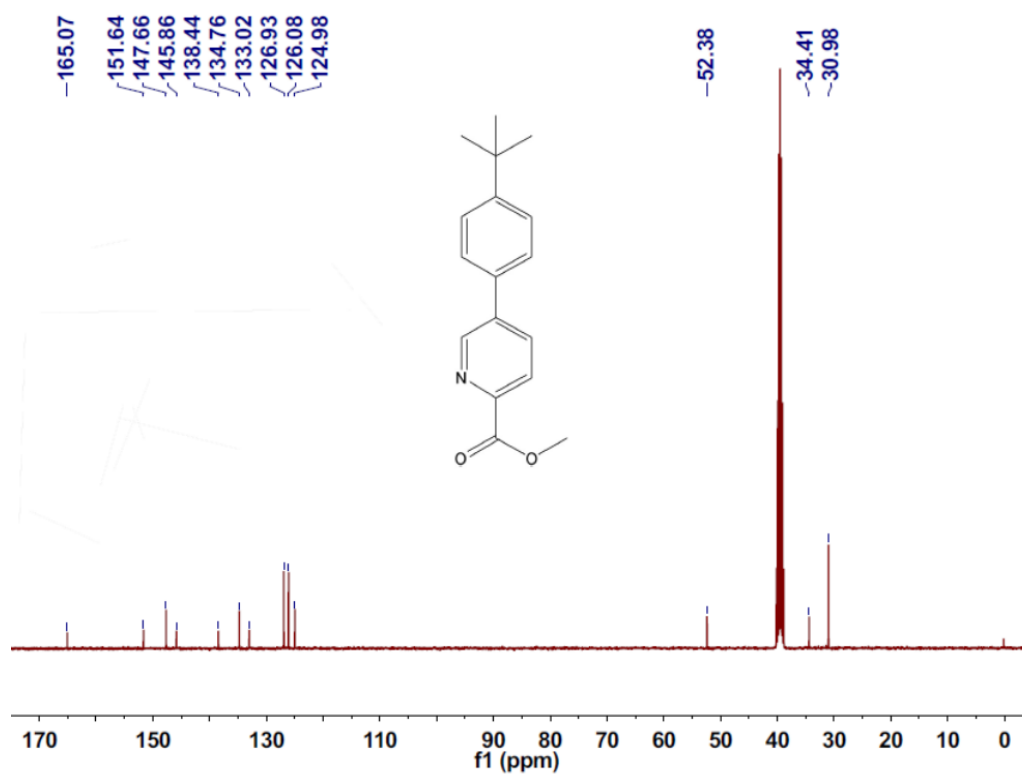


Fig. S18 The ^{13}C NMR spectrum of methyl 5-(4-(tert-butyl)phenyl)picolinate.

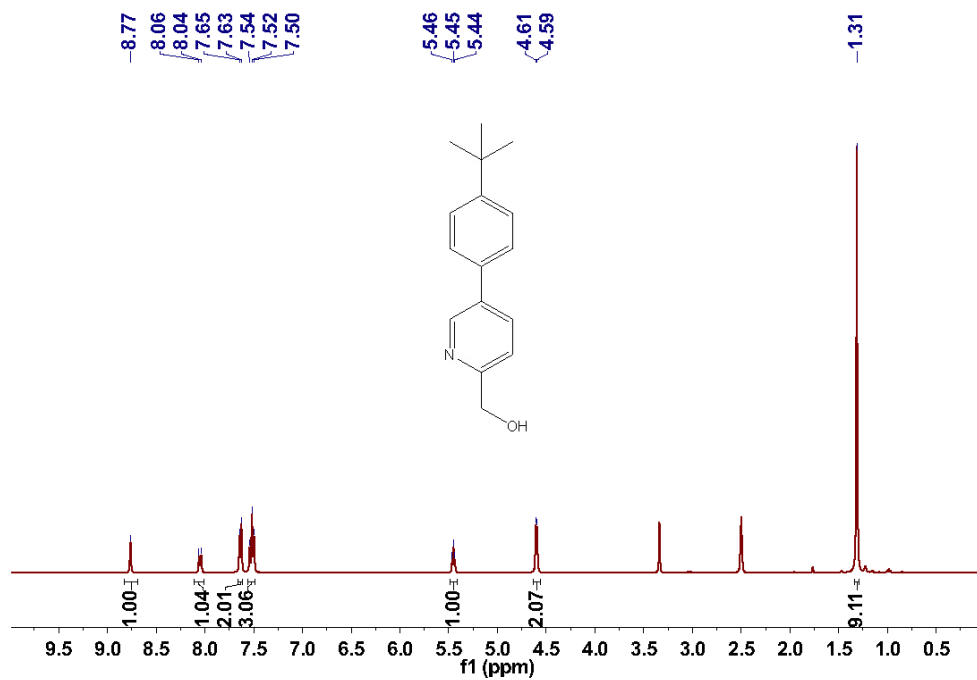


Fig. S19 The ¹H NMR spectrum of (5-(4-(tert-butyl)phenyl)pyridine-2-yl)methanol.

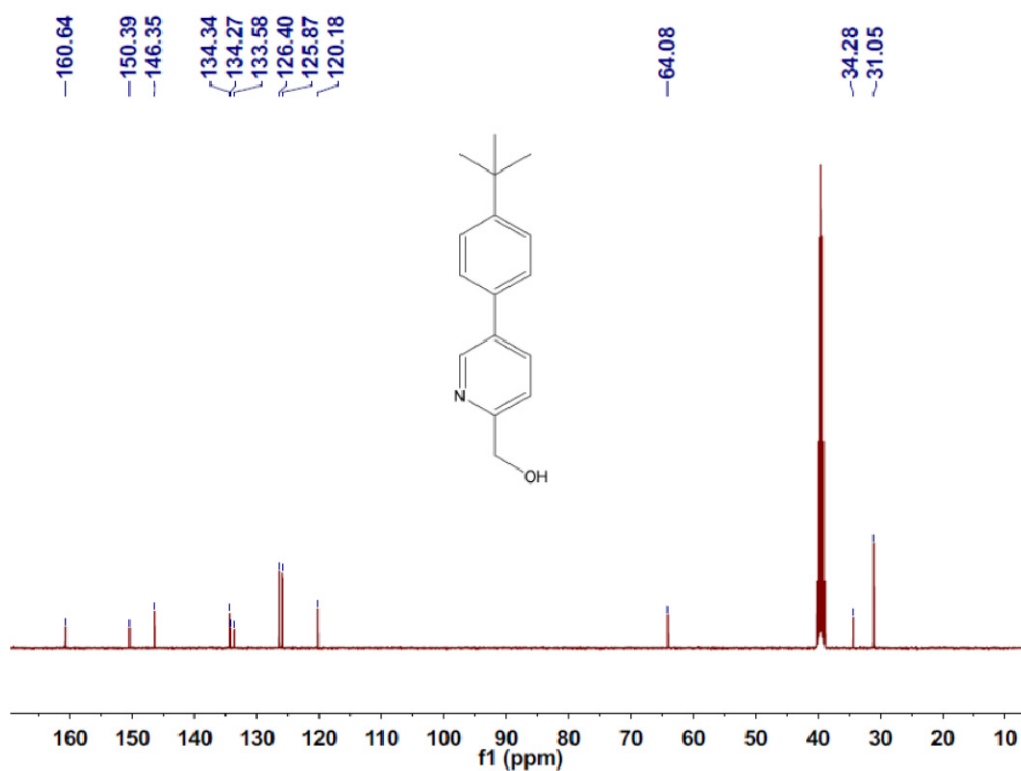


Fig. S20 The ¹³C NMR spectrum of (5-(4-(tert-butyl)phenyl)pyridine-2-yl)methanol.

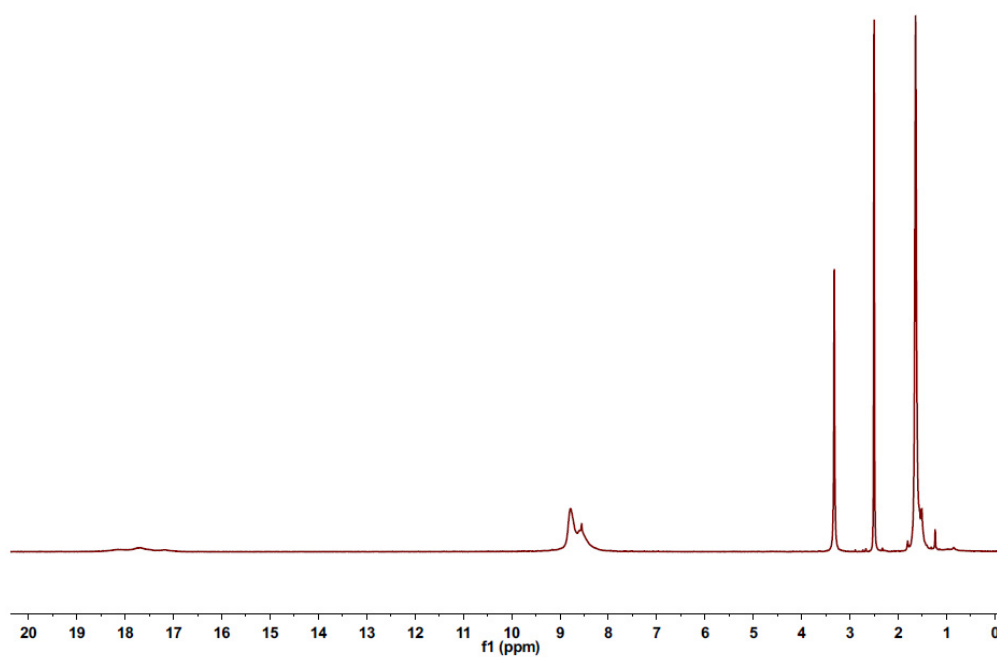


Fig. S21 The ^1H NMR spectrum of compound **1**.

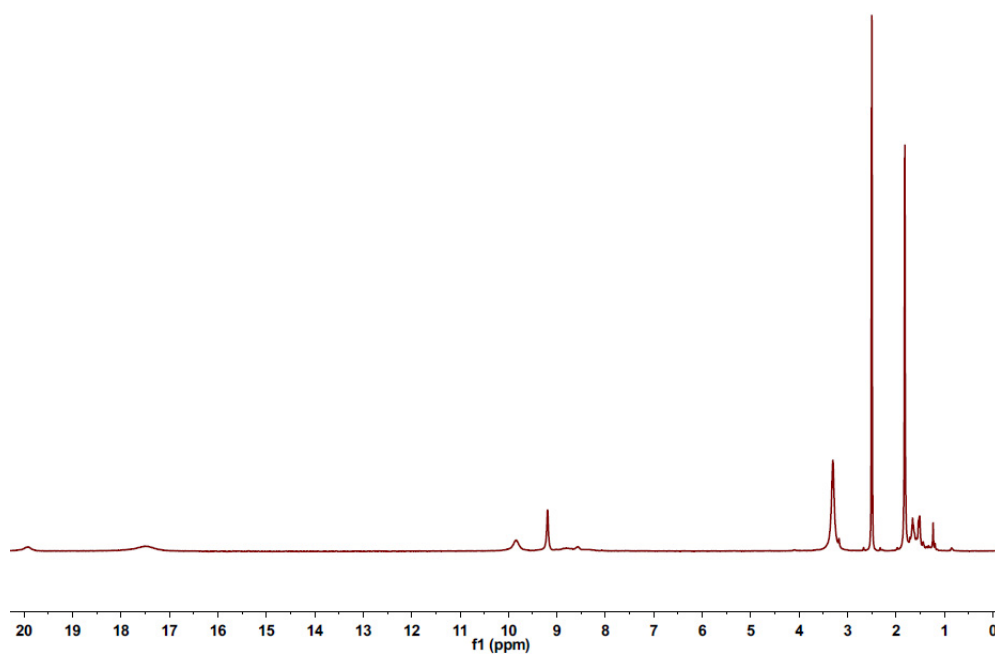


Fig. S22 The ^1H NMR spectrum of compound **2**.

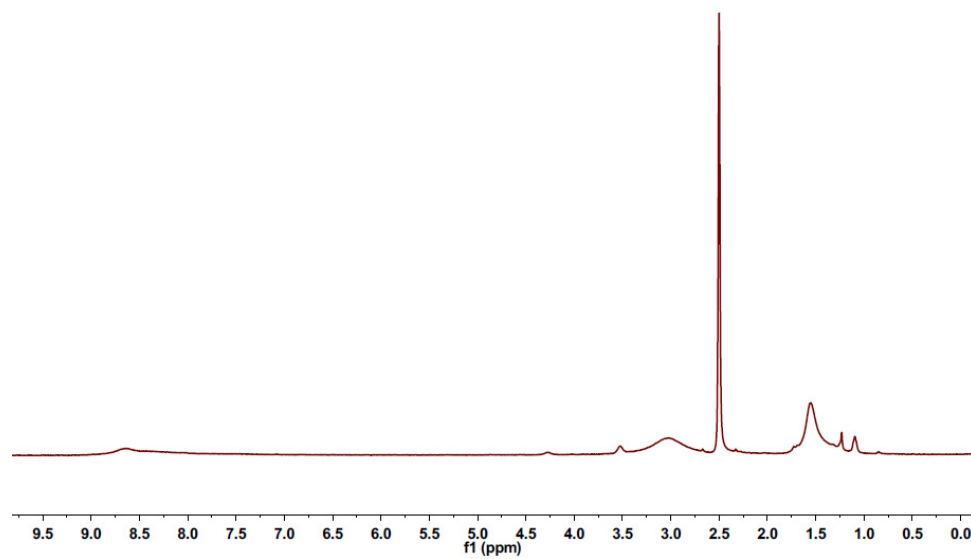


Fig. S23 The ^1H NMR spectrum of compound **3**.

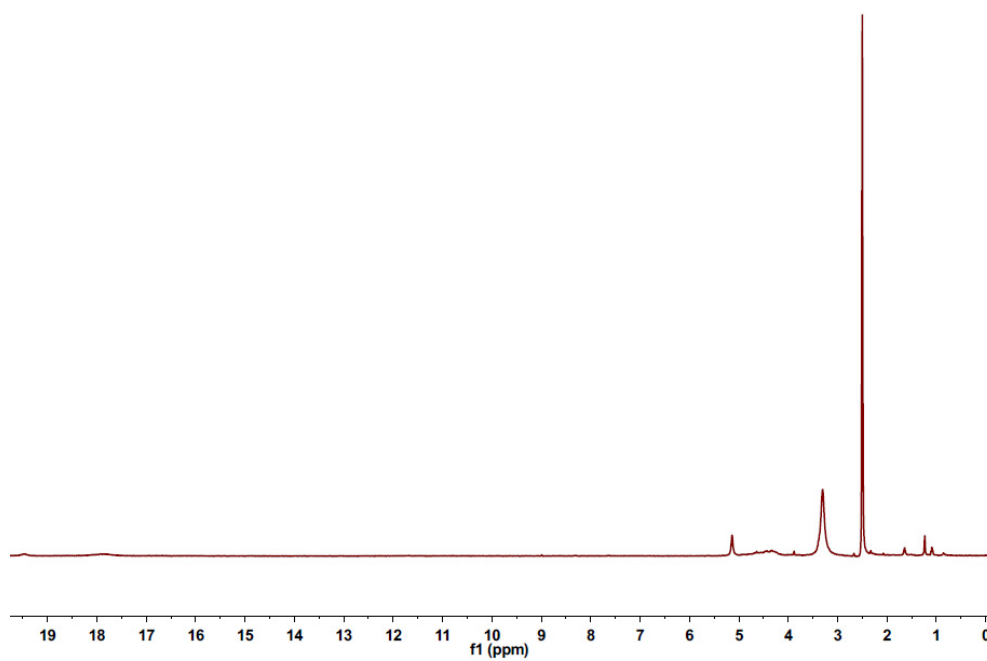


Fig. S24 The ^1H NMR spectrum of compound **4**.

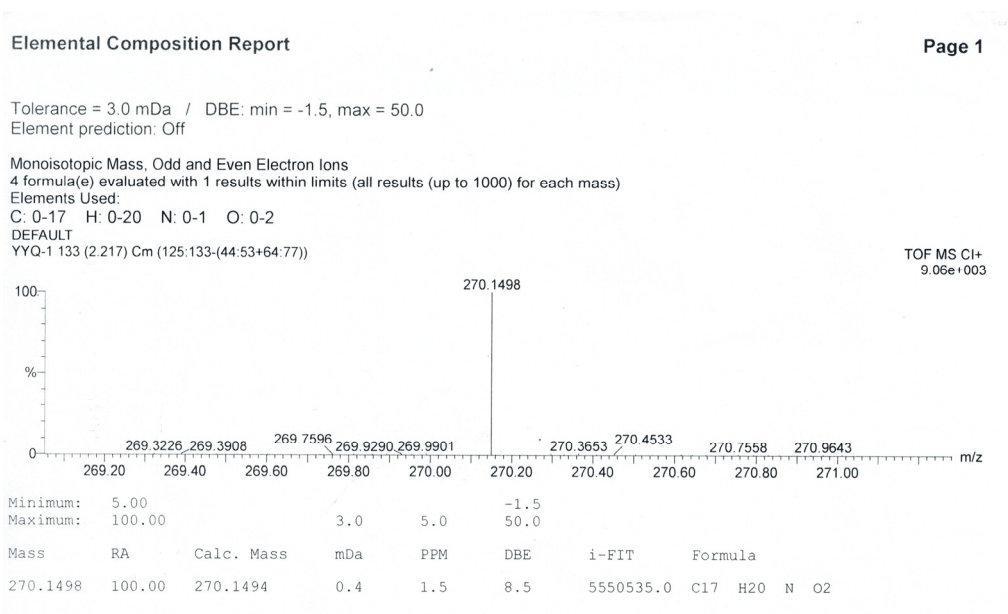


Fig. S25 The TOF-MS spectrum of methyl 5-(4-(tert-butyl)phenyl)picolinate.

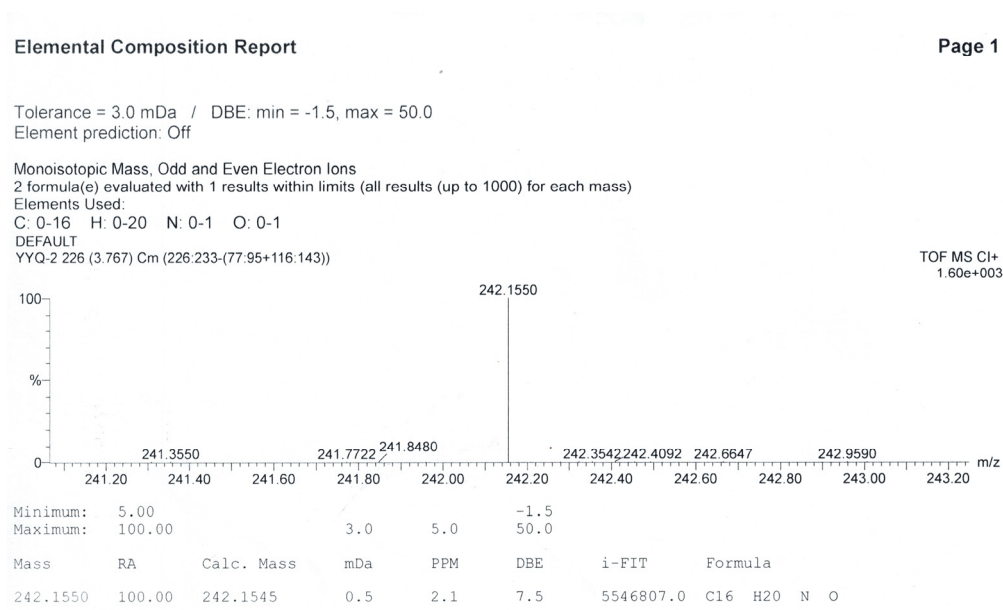


Fig. S26 The TOF-MS spectrum of (5-(4-(tert-butyl)phenyl)pyridine-2-yl)methanol.

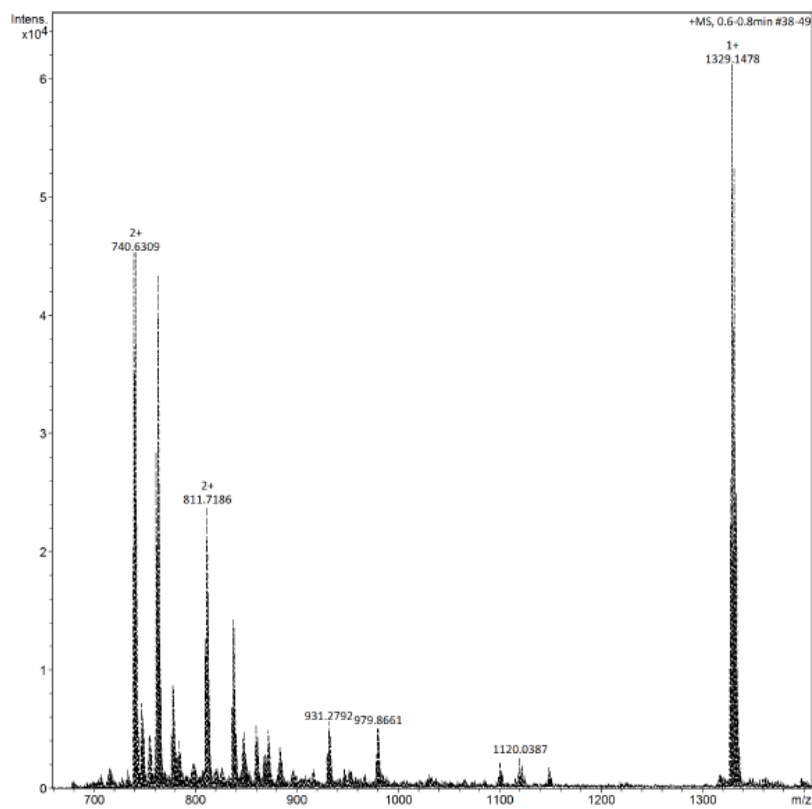


Fig. S27 The ESI-MS spectrum of compound 1.

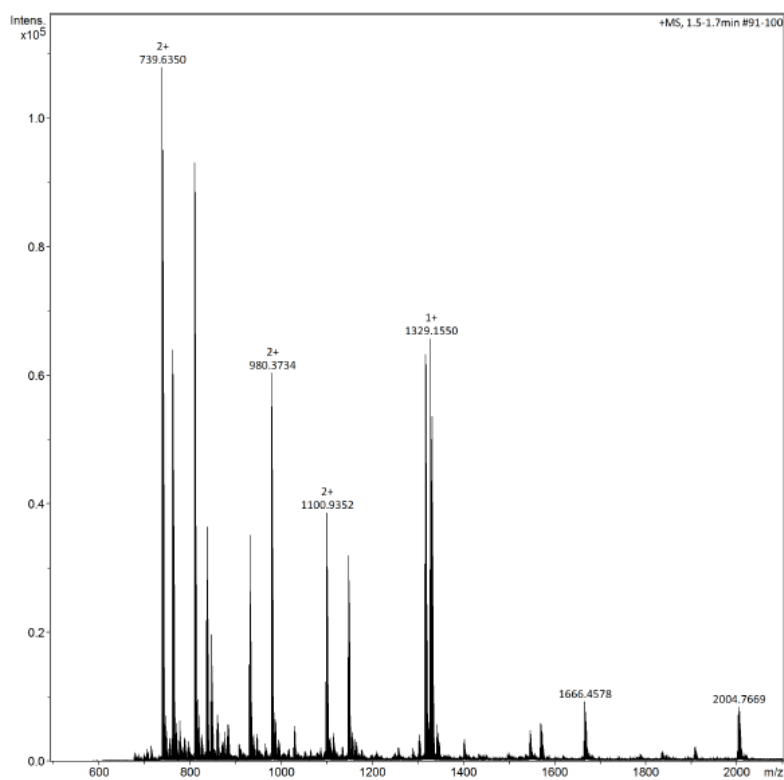


Fig. S28 The ESI-MS spectrum of compound 2.

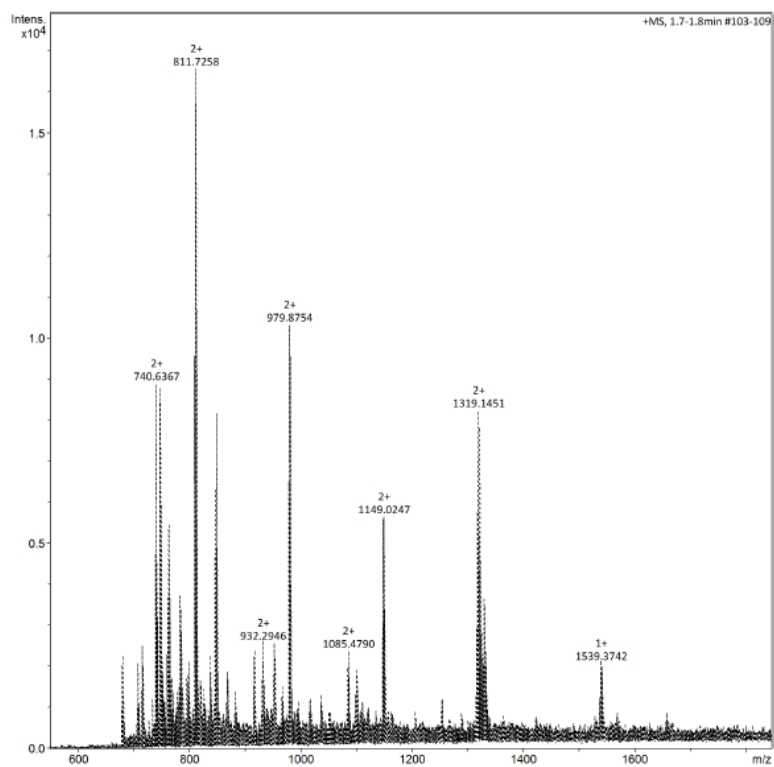


Fig. S29 The ESI-MS spectrum of compound 3.

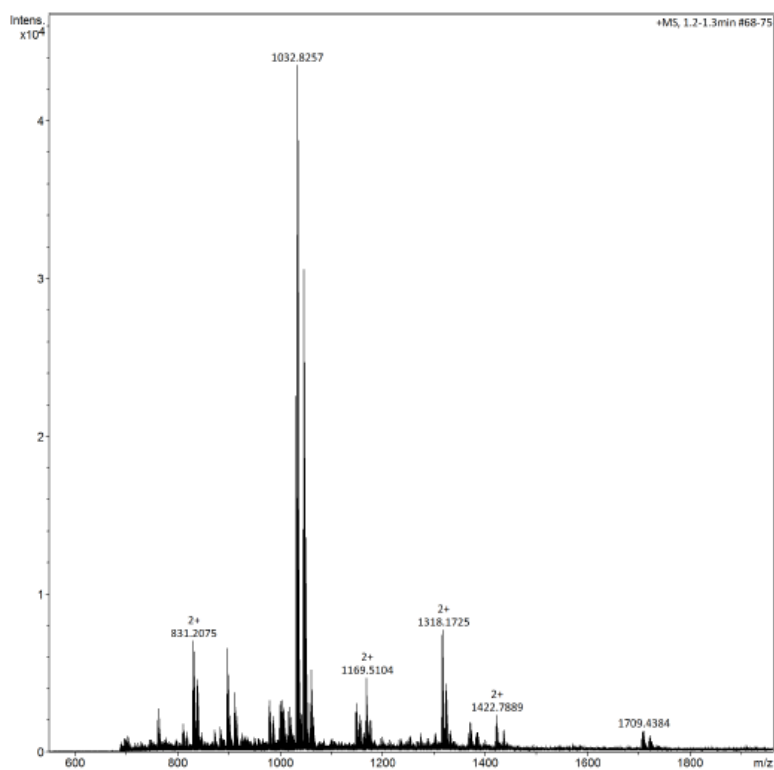


Fig. S30 The ESI-MS spectrum of compound 4.

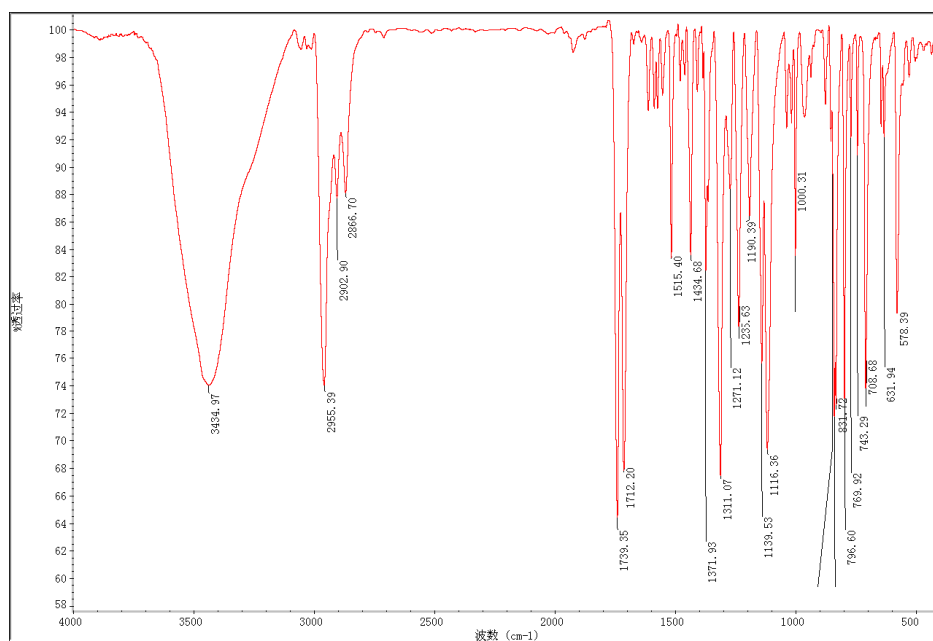


Fig. S31 The IR spectrum of methyl 5-(4-(tert-butyl)phenyl)picolinate.



Fig. S32 The IR spectrum of (5-(4-(tert-butyl)phenyl)pyridine-2-yl)methanol.

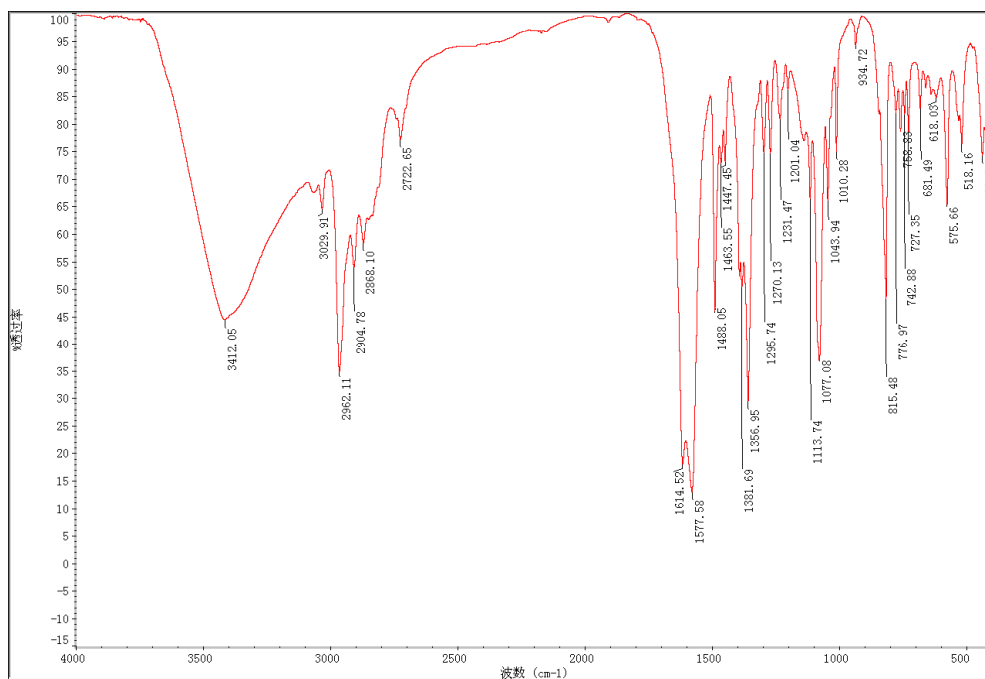


Fig. S33 The IR spectrum of compound 1.

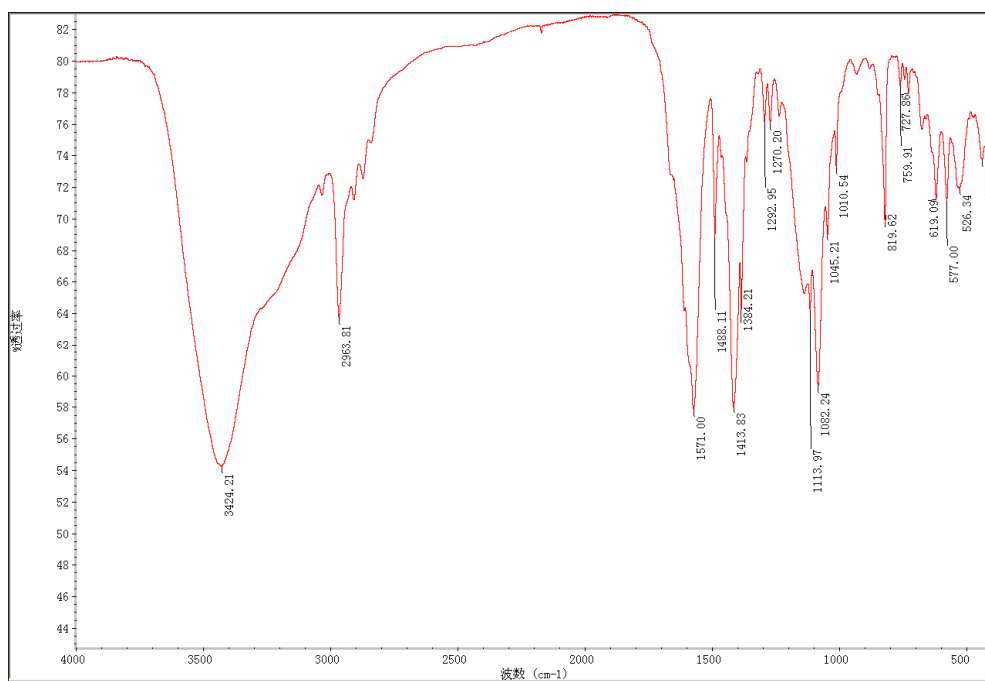


Fig. S34 The IR spectrum of compound 2.

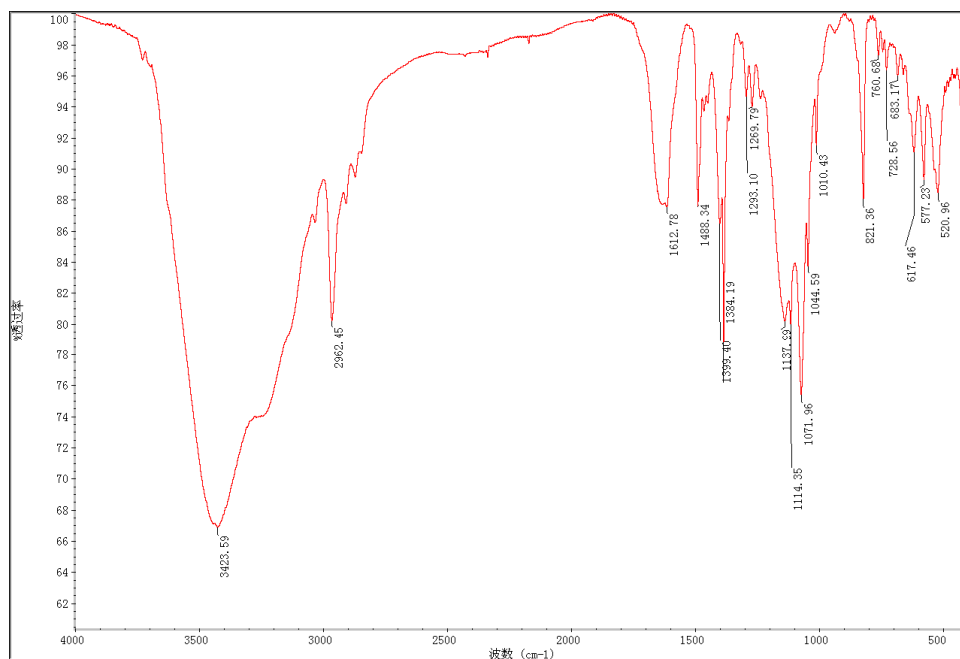


Fig. S35 The IR spectrum of compound **3**.

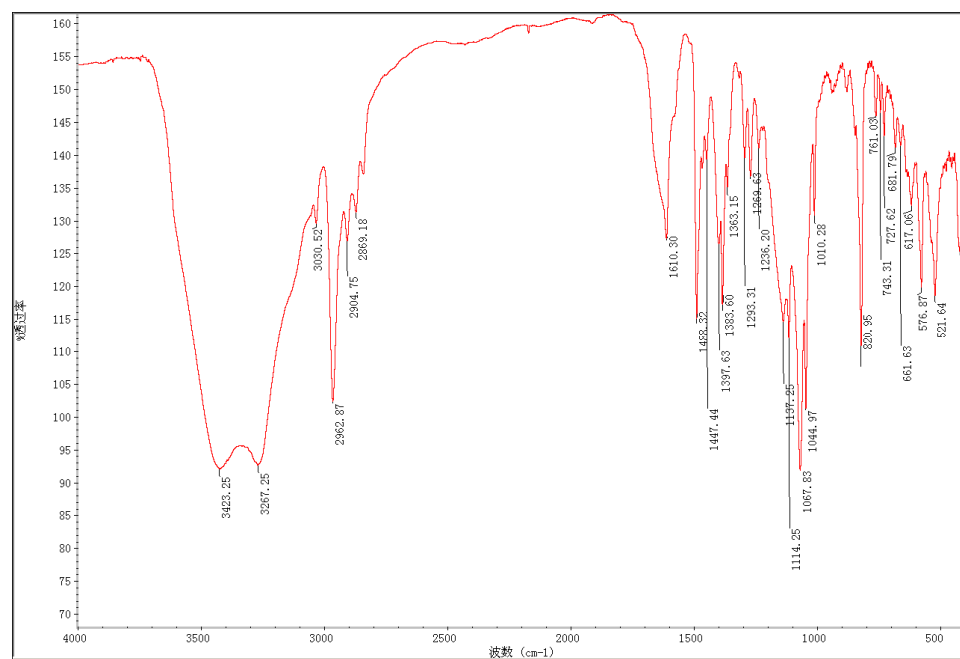


Fig. S36 The IR spectrum of compound **4**.

References

1. M. Armaghan, W. Y. J. Lu, D. Wu, Y. Wei, F.-L. Yuan, S. W. Ng, M. M. Amini, W.-H. Zhang, D. J. Young, T. S. A. Hor and J.-P. Lang, *RSC Adv.*, 2015, **5**, 42978–42989.
2. G. M. Sheldrick, *SADABS, Program for Empirical Absorption Correction of Area Detector Data*; University of Göttingen, Germany, 1996.

3. G. Sheldrick, *Acta Crystallogr., Sect. C*, 2015, **71**, 3–8.
4. L. J. Farrugia, *J. Appl. Cryst.*, 1999, **32**, 837–838.
5. A. L. Spek, *J. Appl. Cryst.*, 2003, **36**, 7–13.
6. Y. Deng, Y. Cai, Z. Sun, J. Liu, C. Liu, J. Wei, W. Li, C. Liu, Y. Wang and D. Zhao, *J. Am. Chem. Soc.*, 2010, **132**, 8466–8473.
7. S. Zhang, S. Gai, F. He, Y. Dai, P. Gao, L. Li, Y. Chen and P. Yang, *Nanoscale*, 2014, **6**, 7025–7032.
8. N. Sahiner, H. Ozay, O. Ozay and N. Aktas, *Appl. Catal., A*, 2010, **385**, 201–207.
9. S. Tang, S. Vongehr and X. Meng, *J. Mater. Chem.*, 2010, **20**, 5436–5445.
10. Z. Jiang, J. Xie, D. Jiang, X. Wei and M. Chen, *CrystEngComm*, 2013, **15**, 560–569.